



HAL
open science

The use of distributed hydrological models for the Gard 2002 Flash-Flood event: Analysis of associated hydrological processes

Isabelle Braud, H el ene Roux, S. Anquetin, Marie-Madeleine Maubourguet, C.
Manus, P. Viallet, Denis Dartus

► To cite this version:

Isabelle Braud, H el ene Roux, S. Anquetin, Marie-Madeleine Maubourguet, C. Manus, et al.. The use of distributed hydrological models for the Gard 2002 Flash-Flood event: Analysis of associated hydrological processes. *Journal of Hydrology*, 2010, 394 (1-2), p. 162 - 181. 10.1016/j.jhydrol.2010.03.033 . hal-00546711

HAL Id: hal-00546711

<https://hal.science/hal-00546711>

Submitted on 14 Dec 2010

HAL is a multi-disciplinary open access archive for the deposit and dissemination of scientific research documents, whether they are published or not. The documents may come from teaching and research institutions in France or abroad, or from public or private research centers.

L'archive ouverte pluridisciplinaire **HAL**, est destin ee au d ep ot et  a la diffusion de documents scientifiques de niveau recherche, publi es ou non,  emanant des  tablissements d'enseignement et de recherche fran ais ou  trangers, des laboratoires publics ou priv es.

1 **The use of distributed hydrological models for the Gard 2002 Flash-Flood event.**

2 **Analysis of associated hydrological processes**

3
4 Isabelle Braud (1), H el ene Roux (2,3), Sandrine Anquetin (4), Marie-Madeleine Maubourguet
5 (2,3), Claire Manus (1,4), Pierre Viallet (5), Denis Dartus (2,3)

6
7 (1) Cemagref, UR HHLY, CP 220, 3bis Quai Chauveau, 69336 Lyon Cedex 9, France

8 (2) Universit e de Toulouse ; INPT, UPS ; IMFT (Institut de M ecanique des Fluides de
9 Toulouse) ; F-31400 Toulouse, France

10 (3) CNRS ; IMFT ; F-31400 Toulouse, France

11 (4) Laboratoire d' tude des Transferts en Hydrologie et Environnement, Universit e de
12 Grenoble (CNRS, UJF, IRD, INPG) (France)

13 (5) HYDROWIDE, 1025 Rue de la Piscine, Domaine universitaire, 38400 St-Martin d'H eres

14
15 This is the author's version of a work accepted for publication by Elsevier. Changes resulting
16 from the publishing process, including peer review, editing, corrections, structural formatting
17 and other quality control mechanisms, may not be reflected in this document. Changes may
18 have been made to this work since it was submitted for publication. A definitive version was
19 subsequently published as

20 Braud, I., Roux, H., Anquetin, S., Maubourguet, M.M., Manus, C., Viallet, P., Dartus D.,
21 2010: The use of distributed hydrological models for the Gard 2002 Flash-Flood event.
22 Analysis of associated hydrological processes, *Journal of Hydrology*, Flash Floods special
23 issue, 394, 162-181, DOI:10.1016/j.jhydrol.2010.03.033

24 <http://www.sciencedirect.com/science/journal/00221694>

1 **Abstract**

2 This paper presents a detailed analysis of the September 8-9 2002 flash flood event in the
3 Gard region (southern France) using two distributed hydrological models: CVN built within
4 the LIQUID[®] hydrological platform and MARINE. The models differ in terms of spatial
5 discretization, infiltration and water redistribution representation, and river flow transfer.
6 MARINE can also account for sub-surface lateral flow. Both models are set up using the same
7 available information, namely a DEM and a pedology map. They are forced with high
8 resolution radar rainfall data over a set of 18 sub-catchments ranging from 2.5 to 99 km² and
9 are run without calibration. To begin with, models simulations are assessed against post field
10 estimates of the time of peak and the maximum peak discharge showing a fair agreement for
11 both models. The results are then discussed in terms of flow dynamics, runoff coefficients and
12 soil saturation dynamics. The contribution of the sub-surface lateral flow is also quantified
13 using the MARINE model. This analysis highlights that rainfall remains the first controlling
14 factor of flash flood dynamics. High rainfall peak intensities are very influential of the
15 maximum peak discharge for both models, but especially for the CVN model which has a
16 simplified overland flow transfer. The river bed roughness also influences the peak intensity
17 and time. Soil spatial representation is shown to have a significant role on runoff coefficients
18 and on the spatial variability of saturation dynamics. Simulated soil saturation is found to be
19 strongly related with soil depth and initial storage deficit maps, due to a full saturation of
20 most of the area at the end of the event. When activated, the signature of sub-surface lateral
21 flow is also visible in the spatial patterns of soil saturation with higher values concentrating
22 along the river network. However, the data currently available do not allow the assessment of
23 both patterns. The paper concludes with a set of recommendations for enhancing field
24 observations in order to progress in process understanding and gather a larger set of data to
25 improve the realism of distributed models.

1

2 **Keywords:** Flash floods, distributed modelling, soil variability, hydrological processes,

3 saturation excess, infiltration excess, model inter-comparison

4

5

6

1 Introduction

2 Flash floods represent the most destructive natural hazard in the Mediterranean region,
3 causing around one billion Euros worth of damage in France over the last two decades
4 (Gaume et al., 2009). Flash floods are associated with extreme and rare rainfall events and
5 usually occur in ungauged river basins. Amongst them, small-ungauged catchments are
6 recognized as the most vulnerable to storm driven flash floods (Ruin et al., 2008).

7 In order to limit damage to the population, there are several currently accepted methods for
8 predicting flash floods in ungauged river basins. The flash flood guidance (Georgakakos,
9 2006; Norbiato et al., 2008) and the discharge threshold exceedance approach (Reed et al.,
10 2007; Younis et al., 2008) are built to give an early flash flood warning with suitable time to
11 organize the civil protection. These operational methods are very efficient for warning, but
12 must be complemented with field experiments and modelling studies to improve the
13 understanding of the major hydrological factors associated with the flood events. In order to
14 progress in process understanding related to flash floods, large scale in situ experiments are
15 scheduled in the context of the HyMeX program (www.hymex.org). This project aims at
16 improving our understanding and prediction of the Mediterranean Sea water balance. The
17 latter can be highly impacted by extreme events which provide a sudden input of fresh water
18 to the sea (Drobinski et al., 2008). One of the focuses of HyMeX is therefore extreme events
19 and, in particular, flash floods over the whole Mediterranean region. The objective is to better
20 understand these events and to improve the predictive capability of hydro-meteorological
21 models in simulating and anticipating them. The quantification of global change impact on the
22 frequency and magnitude of these extreme events will also be analyzed within HyMeX. To
23 achieve these goals, the HyMeX program is planning to enhance the observation capabilities
24 of the scientific community in the Mediterranean region in order to better document extreme
25 rainfall events and flash floods during a ten-year period, with an enhanced period of four

1 years and two special observation periods in the fall. This experimental framework offers a
2 good opportunity to enhance hydrological process observations and understanding. Progress
3 in hydrological modelling of these events are also expected. As all the catchments cannot be
4 surveyed, it is important to determine which type of observations are required and, where and
5 when these observations are needed.

6 Distributed hydrological models, representing physical mechanisms, are interesting tools for
7 hypothesis testing and field design (Loague et al., 2006). Sensitivity studies to process
8 representation, spatial discretization, input data and parameters can be performed that allow
9 the quantification of the impact of various functioning hypotheses on the hydrological
10 response (Pinol et al., 1997, Sangati et al., 2009). Vivoni et al. (2007), using the tRIBs
11 distributed model (Ivanov et al., 2004), explored the complex interactions between the various
12 runoff contributions (infiltration excess, saturation excess, perched return flow, groundwater
13 exfiltration) and the rainfall and catchments characteristics (soil, land use, topography). They
14 showed how various responses can be observed at the outlet according to spatial and temporal
15 variability of these factors and that threshold effects can be observed. Using the same model,
16 Noto et al. (2008) focused on the impact of initial moisture (specified using a variable initial
17 groundwater level) on the catchment response; they highlighted the complexity of the
18 hydrological response to rainfall and soil characteristics. These studies focused on synthetic
19 rainfall events and the studied catchment was about 800 km². Extreme events were not
20 considered in these studies and the analysis was performed for the whole catchment without
21 describing the internal variability.

22 The present paper deals with extreme events at the regional scale and aims at addressing small
23 ungauged catchments ranging from a few km² to about 100 km². In the context of the PUB
24 (Prediction of Ungauged Catchments) initiative, the questions addressed in the paper are the
25 following: i) is it possible to set up physically-based distributed hydrological models at the

1 regional scale using available data and information for flash flood simulation?; ii) are post-
2 flood data of maximum peak discharge useful to assess the relevance of the modelling?; iii)
3 are they relevant to discriminate between various model structures?; iv) are sensitivity studies,
4 based on distributed hydrological models outputs, useful to assess the limits of current
5 observations and highlight which information should be acquired in future field experiments,
6 in order to progress in the understanding and simulation of flash flood events for such
7 catchments. For this purpose, two distributed hydrological models with different model
8 structures are used. The study is conducted for the 8-9th September 2002 event, which affected
9 the Gard region in south-east France. This event was exceptional, both in its extent (more than
10 20000 km² affected) and duration, with more than 600 mm accumulated rainfall in 24 h in
11 some locations. For this event, radar rainfall and post flood field data of maximum peak
12 discharge are available.

13 The case study, rationale for model choice, model description and set up are presented first.
14 The methodology used for model evaluation based on maximum peak discharge and
15 sensitivity studies is also presented. The second part of the paper describes the model results
16 in terms of simulation of maximum peak discharge. This analysis is complemented by local
17 sensitivity studies and a discussion of model results in terms of hydrograph, runoff
18 coefficient, and soil saturation dynamics. After a discussion of the results, guidelines for
19 future experiments are proposed. These includes the processes, variables and parameters that
20 require further description and investigation.

21

1 **Materials and methods**

2 *Case study and available data*

3 The case study is the September 8-9, 2002 event which affected the Gard region located in the
4 South-East of France (Figure 1). This event is the most important event ever recorded in this
5 region. It was responsible for 24 casualties and caused roughly 1.2 million euros worth of
6 damage. This event was extensively described in Delrieu et al. (2005) and in Manus et al.
7 (2009). Thus, we shall only present the data used in the present study. In terms of rainfall
8 input, we used rainfall intensity data from the Bollène radar with a 1x1 km² grid resolution
9 and a 5min time step, with the ST-AD3 processing protocol described by Delrieu et al.
10 (2009). The spatial variability of soils is described using the Languedoc-Roussillon soil data
11 base (later referred as BDSol-LR), provided by INRA (National Institute of Agronomic
12 Research) from the French IGCS (Inventory, Management and Conservation of Soils)
13 program. This database provides information (i.e. texture, horizon depth, etc..) on pedological
14 landscape units called Soil Cartographic Units (SCUs). These units are established with a
15 resolution of 1/250000 and they are geo-referenced. They are composed of Soil Typological
16 Units (STUs), the vertical heterogeneity of which is described by stratified homogeneous
17 layers of soil. The proportion of STUs is given within a particular SCU, but the precise
18 location of STUs within this SCU is unknown. Each STU is described through tables providing
19 both quantitative and qualitative information from which quantities such as percentage of
20 sand, clay, silt, organic matter or soil depth can be derived. Pedo-transfer functions are used
21 to derive the hydraulic parameters of the various soil horizons (see details below).
22 For model evaluation, we use data from an extensive post-flood investigation carried out
23 during the months following the event. The methodology of Gaume and Bouvier (2004) was
24 used during this field survey. The survey gathered a regional information about the flood,
25 allowing the analysis of the hydrological behaviour of watersheds with an area of 2 to 300

1 km². The procedure provides estimation of maximum discharges based on water level marks
2 and simple hydraulic hypotheses for the derivation of the flow velocity. The flood chronology
3 is documented based on witnesses interviews. A sub-set of data corresponding to the same 17
4 sub-catchments, already studied by Manus et al. (2009), is chosen. The area of these
5 catchments ranges from 2.5 to 50 km² (Table 1). In addition, one 99 km² gauged catchment,
6 the Saumane catchment, is also considered. Catchment locations are shown in Figure 1 and
7 their main characteristics are summarized in Table 1. The catchments located in the north-
8 western part of the domain have steep slopes, whereas the catchments located in the south-
9 eastern part of the domain are situated in flatter areas (Figure 1). Table 1 shows a large
10 variability in average soil depth and maximum storage capacity of these catchments. The
11 variables in Table 1 are derived from the BDsol-LR using the dominant STU in each SCU.

12 *Modelling hypotheses and model choice*

13 First of all, the choice of the model should be dictated by the objectives of the modelling
14 exercise (e.g. Kamp and Burges, 2007). Concerning regional flash flood modelling, model
15 requirements are presented in Borga et al. (2008) and Sangati et al. (2009). They underline
16 that “*the space-time excess rainfall distribution and drainage network structure provide the*
17 *most important control on extreme flood response structure*” (Sangati et al., 2009). Therefore,
18 models used in regional flash flood studies should take into account high resolution rainfall
19 and represent soil spatial variability. In order to conduct the study, two distributed
20 hydrological models, able to cope with these requirements, and differing in their structure are
21 chosen. The first model is the CVN (Cévennes) model which is built within the LIQUID[®]
22 hydrological modelling platform (Viallet et al., 2006; Branger et al., 2009¹). The second

¹ Branger, F., Braud, I., Debionne, S., Viallet, P., Dehotin, J., Hénine, H., Nédélec, Y., Anquetin, S., 2009.
Towards multi-scale integrated hydrological models using the LIQUID framework. Overview of the concepts
and first application examples, *Environmental Modeling & Software*, in revision

1 model is the MARINE model, dedicated to flash flood modelling (Maubourguet et al., 2007;
2 Bessière et al., 2008). The two models are representative of the variety of distributed
3 hydrological models used in flash flood event simulation (see references cited by Sangati et
4 al., 2009). In addition and in order to be useful for experimental design, the models must be
5 physically-based so that their inputs parameters and variables, and outputs variables can be
6 related to observable quantities. Kampf and Burges (2007) propose a synthesis and a
7 classification of distributed hydrological models, that highlights the main points which must
8 be considered when describing a model structure. Following this classification, the spatial
9 domain over which the model is applied, the space and time discretization, and the processes
10 which are considered, including surface/subsurface, overland, channel flows, and other
11 processes, as well as their coupling, must be described. These various points are reviewed
12 below for the two models, following the suggestion of Kampf and Burges (2007). Both
13 models are applied at the catchment scale.

14

15 *Models description*

16 MARINE

17 The MARINE model is a spatially distributed rainfall-runoff model dedicated to extreme
18 event simulation and developed on the basis of physical process representation. The model is
19 structured as three physical modules (Figure 2a), which represent vertical transfer (infiltration
20 and runoff generation for the soil component), lateral transfer and both the overland flow
21 component and the flow through the drainage network. Interception and evapotranspiration
22 are not represented since they are considered negligible during individual flood events.

23 The model output is a simulated hydrograph which is available at the catchment outlet but
24 also at any point of the drainage network. It is also possible to follow the evolution of

1 distributed variables such as soil moisture over all the catchment. A description of each model
2 component is detailed hereafter.

3 ***Spatial discretization***

4 The spatial discretization of the catchment is performed using the Digital Elevation Model
5 grid resolution.

6 ***Surface and subsurface flow***

7 Infiltration is described using the Green and Ampt (1911) model, which assumes one-
8 dimensional flow in vertically homogeneous soil columns.

9 The subsurface model is based on Darcy's law. Using the classical assumptions that (i) the
10 slope of the water table in the saturated zone coincides with the local topographic slope, and
11 (ii) the local transmissivity is an exponential function of the local storage deficit (Original
12 TOPMODEL assumption (Beven and Kirkby, 1979)), the flow per unit width q is expressed
13 as:

$$14 \quad q(t) = T_0 \exp\left(-\frac{\theta_s - \theta}{m}\right) \tan \beta \quad (1)$$

15 where T_0 is the local transmissivity of fully saturated soil ($\text{m}^2 \cdot \text{s}^{-1}$), θ_s and θ are the saturated
16 and local water contents ($\text{m}^3 \text{ m}^{-3}$), m is the transmissivity decay parameter (-) and β is the
17 local slope angle (-). Soil water can exfiltrate in two cases: (i) when the soil water content, θ ,
18 exceeds saturated water content θ_s ; (ii) when the soil water reaches the drainage network. It is
19 assumed that exfiltration into the drainage network occurs with a velocity calculated using
20 equation (1). Both infiltration excess and saturation excess are therefore represented within
21 MARINE. In the present study, and in order to allow comparison with the CVN model, the
22 MARINE model is run without activation of the subsurface lateral flow component. In the
23 sensitivity analysis, the impact of including subsurface flow in the modelling is discussed.

24 ***Overland flow and channel flow***

1 The surface runoff is divided into two parts: the overland flow and the flow through the
2 drainage network. Both are simulated using the 1D kinematic wave approximation of the
3 Saint-Venant equations with the Manning friction law. When the drainage area becomes
4 greater than 1 km², the overland flow is structured in a drainage network. Flow in this
5 drainage network takes into account a simplified network reach cross-section (Figure 2b).
6 This leads to a new transport equation in the drainage network. Characteristics of the network
7 reach are calculated using geomorphological considerations (Liu and Todini, 2002): network
8 reach width W_{Di} and depth H_{Di} are taken to increase as a function of the area drained by the i^{th}
9 cell, such that :

$$\begin{aligned} W_{Di} &= W_{Dmax} + \left(\frac{W_{Dmax} - W_{Dmin}}{\sqrt{a_{tot}} - \sqrt{a_{th}}} \right) (\sqrt{a_{di}} - \sqrt{a_{tot}}) \\ H_{Di} &= H_{Dmax} + \left(\frac{H_{Dmax} - H_{Dmin}}{\sqrt{a_{tot}} - \sqrt{a_{th}}} \right) (\sqrt{a_{di}} - \sqrt{a_{tot}}) \end{aligned} \quad (2)$$

11 where W_{Dmax} is the maximum width at the basin outlet, W_{Dmin} is the minimum width,
12 corresponding to the threshold area $a_{th}=1$ km², which is the minimum upstream drainage area
13 required to initiate a channel, a_{tot} is the total area and a_{di} is the area drained by the i^{th} cell.

14 MARINE is run with a fixed time step of 15 s for numerical stability reasons.

15

16 CVN

17 The CVN model is built within the LIQUID[®] modelling platform (Viallet et al., 2006). The
18 system allows a customized model building by assembling process modules described with
19 their own spatial discretization and numerical schemes. These modules can exchange fluxes
20 both in space and time, and the interactions between the various modules are managed by a
21 time sequencer. Each model component is therefore run with an adaptative time step,
22 consistent with its own dynamics. Using the LIQUID[®] modelling platform, model complexity
23 can be increased step by step, allowing a better control and analysis of the impact of various

1 model conceptualizations in terms of hydrological response. In this study, a first –simple-
2 version of the model is used. In particular, as in the MARINE model, interception and
3 evapotranspiration are neglected during the event.

4 ***Spatial discretization***

5 The catchment discretization is based on the principles proposed by Dehotin and Braud
6 (2008) with several levels of discretization. The first level is composed of sub-catchments,
7 organised along the river network (Figure 3). The second level allows the introduction of
8 some spatial heterogeneity within the sub-catchments, and leads to hydro-landscapes that are
9 assumed homogeneous in terms of hydrological response. Rainfall input is also averaged at
10 the scale of the hydro-landscapes. For flash-flood modelling, only soil heterogeneity as
11 described by the pedology map is considered in the hydro-landscape delineation. The result is
12 illustrated in Figure 3. The hydro-landscapes are the elementary units for the modelling of soil
13 infiltration and vertical water redistribution. The hydro-landscapes are vertically discretized
14 into soil horizons with different hydraulic properties.

15 ***Surface and subsurface flow***

16 On each hydro-landscape, the Richards equation is solved using the Ross (2003) method as
17 validated more extensively by Varado et al. (2006) and Crévoisier et al. (2009). The horizons
18 are sub-divided into cells that are 1cm thick for the stability of the numerical scheme. When
19 the topsoil is saturated, ponding is generated. At the bottom of the hydro-landscapes,
20 gravitational or zero flux boundary conditions can be imposed. Subsurface lateral transfer
21 between hydro-landscapes is not considered in this first version of the model.

22 ***Overland and channel flow***

23 Transfer within the river network is performed using the 1D kinematic wave approximation of
24 the St-Venant equation. The network is discretized into river reaches with one reach per sub-
25 catchment (Figure 3). The river section is assumed trapezoidal with geometrical parameters

1 assigned according to the Strahler order. At this development stage of the model, the routing
2 scheme allowing the transfer of ponding generated on the hydro-landscapes to the river
3 reaches is very simple, as we are focusing on peak discharge and risk assessment,. The
4 ponding is quasi-instantaneously transferred to the closest river reach. The implications of
5 these simplifying hypotheses have been discussed by Manus et al. (2009) (see interactive
6 discussion) and are thus not repeated here.

7 *Model set up*

8 In order to be able to quantify differences and similarities in hydrological responses between
9 the two models, the same input data were used whenever possible. No calibration is
10 performed and both models are run using the a priori information and expert knowledge on
11 the various models derived from previous studies or model user expertise. These simulations
12 will be referred to as the reference simulations in the following of the paper.

13 *Spatial discretization*

14 Both models rely on Digital Elevation Model (DEM) data for river network and sub-
15 catchments delineation. The same 75 m resolution DEM, provided by IGN is used.

16 For the CVN model, the D8 algorithm (e.g. Tarboton, 1997) is used to define the drainage
17 direction map, the cumulated drainage area and the river network. A minimum drainage area
18 of 0.1 km^2 is used to distinguish between network and hillslope pixels. The Strahler order one
19 sub-catchments are considered for the definition of the first level of discretization (Figure 3).
20 This ensures that the hypothesis of instantaneous transfer of ponding to the closest river reach
21 is acceptable. For each river reach, the average slope is computed from the DEM slope
22 information. Unfortunately, the DEM information is truncated to 1 m in height, which can
23 sometimes lead to zero or very small slopes. This is corrected by assigning a minimum slope
24 of 0.5 m (half the vertical DEM resolution) divided by the river reach length.

1 This problem of DEM resolution is much more problematic for the MARINE model which
2 requires a continuity of flow at the scale of the DEM grid. To avoid problems, the DEM is
3 used with a 150 m resolution in MARINE. It is processed to identify connections between
4 cells, leading to the determination of the catchment extent and the flow pathways. DEM data
5 also allow the retrieval of hillslopes and cumulated drainage area, the drainage network and
6 the geometric characteristics of the network reaches. Drainage network extreme widths and
7 depths are derived from in situ measures. As in many rainfall-runoff models (Liu and Todini,
8 2002), drainage is only possible to the North, East, South or West for the four adjacent cells at
9 each edge in MARINE (D4 algorithm).

10 Figure 4b shows the 30 h accumulated rainfall over the catchments. Rainfall is distributed at
11 the pixel scale within MARINE and at the hydro-landscape scale within CVN.

12 *Surface and subsurface flow*

13 For the specification of soil characteristics, the same pedology map, from the BDsol-LR is
14 used by both models. As mentioned above, several Soil Typological Units (STUs) can be
15 present within the Soil Cartographic Units (SCUs). In the present study, the dominant STU
16 within each SCU was assumed representative of the whole SCU. A common map of soil
17 depth and soil texture was built using this information.

18 Within MARINE, soils are assumed to be vertically homogeneous. Soil classes are assigned
19 according to the Rawls and Brackensieck (1983) soil classes according to their texture. For
20 each soil class, a set of parameters (saturated water content, soil suction for the Green and
21 Ampt model and saturated hydraulic conductivity) is assigned.

22 Within the CVN model, the vertical heterogeneity of the soil is considered and the soil
23 hydraulic parameters of the Brooks and Corey (1964) retention and hydraulic conductivity
24 curves are calculated as continuous functions of soil texture and soil porosity using the Rawls
25 and Brackensieck (1985) pedo-transfer function (see details in Manus et al., 2009). A

1 correction of soil saturated water content and hydraulic conductivity which takes into account
2 the stones content was proposed by Manus et al. (2009). This correction is applied to both the
3 CVN and MARINE parameters in the present study.

4 Figure 4a provides an illustration of the resulting variability in terms of maximum storage
5 capacity (calculated as the sum, over all the horizons, of soil saturated water content
6 multiplied by the horizon depth) amongst the studied catchments (Table 1). The range
7 amongst the catchments is very large from about 60 mm to 370 mm.

8 The initial soil moisture is specified based on the SAFRAN-ISBA-MODCOU model with a
9 8x8 km² resolution as provided by Météo-France (Habets et al., 2008). For MARINE, soil
10 parameters and initial soil moisture are distributed at the pixel scale. For the CVN model, soil
11 parameters are distributed at the hydro-landscape scale and initial soil moisture at the
12 catchment scale. Figures 4c and 4d show the spatial variability of initial soil water storage
13 deficit (maximum storage capacity – initial soil water storage) for both the CVN and
14 MARINE models. Table 1 provides a summary of the maximum and initial water storage and
15 deficit per catchment. Initial soil water storage deficits are comparable between the models
16 with slightly lower values for MARINE than for CVN (-7%). Figures 4c and 4d show that
17 CVN exhibits a higher spatial variability of initial water storage deficit than MARINE due to
18 the use of continuous pedo-transfer functions. The CVN and MARINE model are run with a
19 zero flux bottom boundary condition.

20 ***Overland and channel flow***

21 For the flow routing, a constant value of the Manning coefficient of 0.05 is used within the
22 CVN model (Manus et al., 2009).

23 For its overland flow routing, the MARINE model requires the specification of a roughness
24 coefficient. It is derived from a vegetation and land-use map (2000 Corine Land Cover
25 provided by the Service de l'Observation et des Statistiques (SOeS) of the French Ministry of

1 Environment, www.ifen.fr). For the drainage network flow simulation within MARINE, two
2 Manning coefficients, corresponding to the main channel and the floodplain, must be
3 prescribed. They are taken from previous studies on the Gardons d'Anduze catchment with
4 values of 0.05 for the Manning roughness coefficient within the main channel and 0.125
5 within the floodplain (Bessière, 2008).

6 To conclude this section, the major similarities and differences between both model structures
7 are highlighted, based on the criteria proposed by Kampf and Burges (2007).

8 ***Spatial discretization***

- 9 - The model discretizations are different. It is based on grid squares for MARINE and
10 on homogeneous hydro-landscapes for CVN, with irregular polygonal shapes.
- 11 - Radar 1x1 km² and 5 min time step data are interpolated at the DTM grid scale within
12 MARINE and at the hydro-landscape scale within CVN.

13 ***Surface and subsurface fluxes***

- 14 - In terms of soil description, both models rely on the same soil depth and soil texture
15 map, but the soil parameters are specified more coarsely in MARINE than in CVN
16 (soil classes versus continuous pedo-transfer functions). Furthermore, the MARINE
17 model assumes vertically homogeneous soils, whereas CVN accounts for vertical
18 heterogeneity.
- 19 - Soil infiltration is described using the simplified Green and Ampt model in MARINE
20 whereas the 1D Richards equation for saturated/unsaturated flow is used in CVN.
21 CVN also explicitly accounts for water redistribution within the soil layers.
- 22 - Subsurface lateral flow is not considered in the intercomparison of both models

23 ***Overland and channel flow***

- 1 - MARINE includes an hillslope overland flow module, based on the kinematic wave
2 approximation of the de St-Venant equations, whereas CVN uses an empirical
3 approach for overland flow routine
- 4 - In terms of river network, the MARINE discretization is finer and defined at the pixel
5 scale, whereas homogeneous properties per river reach are assumed in CVN.
- 6 - The river section descriptions are also different and MARINE makes the distinction
7 between the main channel and the floodplain, whereas only the main channel in
8 considered in CVN. Both models use the kinematic wave approximation of the de St-
9 Venant equations for the flow routine module.

10 *Other processes and time discretization*

- 11 - Both models are run in this study as event-based models. A variable adaptative time
12 step is used in CVN and a fixed time step is used in MARINE
- 13 - Both models neglect interception and evapotranspiration processes during the extreme
14 rainfall event
- 15 - Both models use the finite volume approach for the numerical solution

16 The two models differ in terms of spatial discretization and have quite similar approaches in
17 terms of soil infiltration representation, with a more refined representation within CVN. Both
18 models differ in terms of water transfer, both within the hillslopes and river network, with a
19 more refined scheme within MARINE.

20

21 *Model evaluation and sensitivity studies*

22 The simulations are conducted from 2002/09/08 at 06hUTC to 2002/09/09 at 12hUTC,
23 corresponding to the rainfall event duration.

24 Firstly, the performance of the models (reference simulations) is assessed at the regional scale
25 using maximum peak discharge data collected during a post-flood field survey. As the models

1 are not calibrated (reference simulation), a global sensitivity analysis to model parameters is
2 conducted in order to assess the uncertainty of the model estimates. Previous global
3 sensitivity studies, using the Monte-Carlo technique, have allowed determination of the most
4 sensitive parameters in MARINE for flash floods (Le, 2008). Their number is limited using
5 the method proposed by Refsgaard (1997) where, for distributed parameters, a spatial pattern
6 is fixed and the considered parameter is a multiplicative factor of the reference map. Three
7 sensitive parameters are identified by Le (2008): a multiplicative factor for the spatial pattern
8 of soil thickness, a multiplicative factor for the spatial pattern of hydraulic conductivity and
9 the roughness coefficient of the floodplain. When lateral subsurface flow is considered, an
10 additional sensitive parameter is the multiplicative factor for the spatial pattern of saturated
11 transmissivity. Based on these conclusions, a global sensitivity analysis is performed for both
12 models for the September 2002 event using the latin hypercube method (see for instance van
13 Griensven et al., 2006 for a review of sensitivity analysis methods) with 20 intervals for each
14 parameter. Four parameters, namely a multiplicative factor for saturated hydraulic
15 conductivity, a multiplicative factor for soil depth, the Manning coefficient (main channel for
16 CVN and flood plain for MARINE, as previous sensitivity studies (Le, 2008) showed that the
17 Manning coefficient for the main channel is not sensitive in MARINE), and the initial
18 saturation are considered in the analysis. Based on expert knowledge in the region, the range
19 and distributions presented in Table 2 are assigned to the various parameters. The target
20 variables in this sensitivity analysis are the maximum specific peak discharge, time of peak,
21 and the runoff coefficient of the various catchments. The impact of rainfall description has
22 been studied in other papers (e.g. Carpenter and Georgakakos, 2004; Teztlaff and
23 Uhlenbrook, 2005; Chancibault et al., 2006; Cole and Moore, 2008; Saulnier and Le Lay,
24 2009) and is not considered here where we focus more on the impact of the description of
25 soil spatial variability and river flow.

1 Secondly, as the results of both models are quite similar in terms of simulation of maximum
2 peak discharge and runoff coefficient, a comparative analysis of both model results is
3 performed in terms of discharge and soil saturation dynamics, in order to see if differences in
4 model behaviour can be identified. This analysis is complemented by local sensitivity studies
5 on some parameters, and studies of the impact of various model structural choices
6 (homogeneous versus distributed soils with CVN, inclusion of subsurface flow in MARINE).

7 **Results**

8 *Model evaluation using post flood event data*

9 Figure 5a shows the comparison of simulated maximum peak discharge with the field
10 estimates (including their uncertainty). Results are summarized in Table 3 which also
11 provides information on the peak discharge time, as derived from witness interviews when
12 available. Figure 5a shows that MARINE simulated values are in general lower than the field
13 observations, whereas CVN simulations tend to be higher. For both models, the peak
14 discharge is overestimated for catchment #10 and #18. Rainfall estimation was found very
15 uncertain for catchment #10, with krigged rainfall gauges leading to a cumulative value of
16 161 mm whereas the radar value was 339 mm. Catchment #18 is discussed in more detail
17 below, as an hydrograph is available. When catchments #10 and #18 are excluded, the root
18 mean square error is $112 \text{ m}^3 \text{ s}^{-1}$ for MARINE and $96 \text{ m}^3 \text{ s}^{-1}$ for CVN and the correlation
19 coefficient between simulated and field values is $R^2=0.95$ for CVN with a slope of 1.14, and
20 $R^2=0.92$ for MARINE with a slope of 0.94. The performance of both models is thus
21 satisfactory with regards to maximum peak discharge uncertainty.

22 Figure 5b shows the comparison between simulated and field estimates of maximum specific
23 peak discharge. The catchments are ordered with increasing area. We can see that maximum
24 specific peak discharge tends to decrease with catchment area. Both models follow this trend.

1 MARINE (respectively CVN) estimates are within the range of uncertainty for 8 (respectively
2 9) catchments over 18, which is satisfactory for such events. If catchments #10 and #18 are
3 excluded, the root mean square error is $6.4 \text{ m}^3 \text{ s}^{-1} \text{ km}^2$ for MARINE and $6.7 \text{ m}^3 \text{ s}^{-1} \text{ km}^2$ for
4 CVN. As for maximum peak discharge, CVN tends to overestimate maximum specific
5 discharge, whereas MARINE tends to underestimate it.

6 For catchment #18, a measured hydrograph is available, but the uncertainty in the measured
7 peak is large (Table 3). The comparison of the simulated and observed hydrographs is
8 provided in Figure 8f. The simulated hydrographs are very similar for both models. Both
9 models overestimate the runoff volume and peak, the overestimation being larger for CVN.

10 For this catchment, located the farthest from the radar, there may be some uncertainty on the
11 rainfall estimate. A deeper analysis of rainfall estimates shows a cumulative rainfall of 208
12 mm with the radar data used in this study, 207 mm with the krigged rain gauges and only 145
13 mm with the data issued from the radar operational treatment. The observed runoff is 85 mm
14 and Table 1 shows that the maximum storage capacity of the catchment is only 68 mm.

15 Therefore, even if the catchment was completely dry, the rainfall should not exceed $85 + 68 =$
16 153 mm to be consistent with the observed runoff. If we take into account uncertainty in the
17 observed runoff by applying a multiplicative factor equal to the ratio of the upper bound to the
18 most probable peak discharge $1050/770 = 1.36$, the “observed” runoff estimation reaches 116
19 mm. Thus, the runoff plus storage only reaches $116 + 68 = 184 \text{ mm}$, which is still below the
20 estimated radar rainfall that we use (208 mm). The alternative hypothesis is an
21 underestimation of catchment maximum storage capacity from the pedology map or the non-
22 imperviousness of the bedrock.

23 These hypotheses and the robustness of the model estimates are examined more in details
24 below using the global sensitivity analysis.

25

1 *Global sensitivity analysis for the simulation of peak discharge and runoff coefficient*

2 The results of the global sensitivity analysis in terms of maximum specific discharge and
3 runoff coefficient are summarized in Figure 6 for both models. Almost none of the parameter
4 set is able to simulate the observed values of maximum specific discharge for catchments #10
5 and #18. It gives more credence to the hypothesis of a problem with rainfall estimation. For
6 catchment #18, only two parameters sets, associated with multiplicative factors of 8.1 (resp.
7 2.1) for saturated hydraulic conductivity, and of 3.6 (resp. 9.4) for soil depth, associated with
8 dry initial conditions (0.11 and 0.34 respectively) are able to provide Nash efficiency values
9 larger than 0.7 for both models. The high values of these multiplicative factors also
10 questioned the relevance of the information provided by the soil data base about soil depth
11 and the pedo-transfer functions used for the estimation of soil hydraulic properties. Enhanced
12 *in situ* measurements of these properties are therefore required.

13 Figure 6 confirms the tendency observed in Figure 5 of an overestimation of maximum peak
14 discharge by CVN and an underestimation by MARINE. For both models, the uncertainty
15 range of the maximum specific peak discharge is in general within the error bounds of the
16 post field data. For the catchments which are poorly simulated by CVN (#3, 7, 8, 10, 15 to 18)
17 or MARINE (#1, 4, 5, 8, 10, 12, 16 to 18), the parameter uncertainty bounds are generally
18 outside the errors bounds of the observed values. In terms of peak discharge (not shown), the
19 time amplitude is small (less than 20 min, except when there are several peaks). When there is
20 a peak of high rainfall intensities (larger than 100 mm hr^{-1}), the time of the peak is very stable,
21 showing that these high rainfall intensities are probably very influential on the peak discharge,
22 especially for the CVN model. For the CVN model, spurious rainfall intensity peaks might be
23 the reason for the general overestimation on the badly simulated catchments. These rainfall
24 peaks are likely to generate infiltration excess runoff, which is instantaneously transferred to
25 the river network. Within the MARINE model, overland flow can smooth the impact of these

1 rainfall peaks. For CVN, the reference simulation is in general very close to the median
2 (Figure 6a), whereas it is closer to the 25th quartile for MARINE.

3 In terms of runoff coefficient, the similarity between both model response is large (Figure 6c
4 and d). The large values of the median runoff coefficient for both models must be highlighted.
5 The CVN 95% interval for the runoff coefficient is in general closer to a runoff coefficient of
6 1 than MARINE. Only some simulations (in general associated with the largest multiplicative
7 factors for soil depth) lead to small values of the runoff coefficient. Figure 7b to d show the
8 relationship between the runoff coefficient and the multiplicative factors for saturated
9 hydraulic conductivity, soil depth and with initial saturation for catchment #15, which is
10 representative of the other catchments. Both models present similar patterns, although the
11 absolute values are different (see next section). This shows that, despite the differences in
12 terms of surface and subsurface representation, the signature of the difference in model
13 structure is weak in terms of runoff coefficient patterns. For the September 2002 extreme
14 event, with an exceptionally large rainfall amount, a generalized soil saturation is simulated
15 for most of the parameter sets. Neither the maximum peak discharge, nor the runoff
16 coefficient allow the identification of significant differences in responses corresponding to
17 differences in model structures for the runoff production components.

18 Figure 7a illustrates the dependence of the simulated maximum peak discharge as a function
19 of the Manning coefficient for catchment #15, but the pattern is similar for the other
20 catchments. For both models, when the Manning coefficient is increased (in log scale), an
21 linear decrease of the maximum peak discharge is simulated. The slope of the relationship is
22 smaller for MARINE than for CVN, showing a lower sensitivity of MARINE to this
23 parameter. This also reflects the fact that MARINE distinguish between the main channel and
24 the floodplain. The reference simulation values are quite different between both models,
25 reflecting different choices in the flow routing and parameter values. When compared to the

1 observed maximum peak discharge (horizontal lines), a range of more plausible values can be
2 highlighted. But the results are different according to the catchments (not shown). The
3 determination of a regional value for the Manning coefficient, based only on the maximum
4 peak discharge appears difficult.

5 In conclusion, given the available information and the uncertainty, both models perform
6 satisfactorily for a wide range of catchment sizes and rainfall input amounts. The results of
7 the global sensitivity analysis show that differences in model structures are not reflected in
8 differences in runoff coefficients. They are partly reflected in differences in maximum
9 specific discharge, but this variable is not sufficient to assess the most suitable model
10 structure. In the remaining of the paper, we go a step further by comparing the model results
11 in terms of simulated process dynamics (discharge and soil saturation) in order to see if
12 information on other variables could help determining which model structure better represents
13 actual processes. The reference simulation is used for this purpose.

14 Nevertheless, we would like to stress the value of post flood field data of maximum peak
15 discharge, as they are the only data available to assess model performance at the regional
16 scale and for catchment areas less than 100 km². In Bonnifait et al. (2009), their Figure 6
17 shows that in the studied region, gauged catchments are only available for areas larger than
18 100 km². Observed hydrographs are of course valuable to verify the simulated flow dynamics
19 for extreme events. However, discharge estimation remains very uncertain for extreme events
20 as stage-discharge relationships are often extrapolated far beyond the maximum gauged value
21 ,and only a few locations are gauged.

22

23 *Catchment hydrological response and flow dynamics*

24 Figure 8 provides the simulated hydrographs by both models for some selected catchments.
25 The horizontal bars show the post flood field estimates of peak discharge and their

1 uncertainty. When available, the times of the peak as stated by witnesses are shown as
2 crosses. Table 3 shows the comparison between simulated and field estimates of peak
3 discharge and time of peak for both models. Figure 8 shows that the shape of the simulated
4 discharge is highly related to the rainfall dynamics with peaks in general associated with high
5 rainfall intensities. The CVN model tends to be more reactive to rainfall than the MARINE
6 model and shows more pronounced peaks than MARINE, with sometimes a large
7 overestimation (#3, #7, #8, #16). It should be noted that MARINE also overestimates the
8 peaks for these catchments (except #3). Differences in model responses increase with
9 increasing size of the catchment (Figure 8) with less pronounced peaks with MARINE than
10 with CVN as long as the catchment area increases. The differences in the transfer modules
11 lead to a larger smoothing of the hydrological response in MARINE than in CVN when the
12 catchment size increases. These differences can be partly related to the transfer module and
13 the difference in the Manning coefficient as shown in Figure 9 and Table 4, and confirmed by
14 the global sensitivity analysis (Figure 7a). When the Manning coefficient is increased from
15 0.05 to $0.125 \text{ m}^{-1/3} \text{ s}^{-1}$, the peak discharge decrease by 16-36% in CVN and by 7-30% in
16 MARINE. The time of peak is delayed by 10-30 min in CVN and by 20-30 min in MARINE.
17 The case of #17 is particular: two peaks are simulated and the change in roughness produces a
18 change of the maximum peak in MARINE which leads to an 11h30 hour difference. Figure 9
19 and Table 4 show that, in general, peaks occur in MARINE before they do in CVN when
20 both models use the same roughness. This is certainly a consequence of the differences in
21 flow routing representations (as both models behave similarly in terms of runoff generation).
22 Figure 9 also shows that with identical roughness coefficients, the response of MARINE
23 remains smoother than that of CVN. In particular, the decrease in peak discharge is less
24 pronounced in MARINE which may be a consequence of the accounting of hillslope transfer
25 within MARINE.

1 When information about the peak hour is available, model estimates agree fairly well with the
2 values provided by the witnesses (or observation for Saumane), with a difference of less than
3 30 min for #1 (second peak), #6, #9, #17 and #18. Differences in peak time estimates can
4 reach more than one hour for #1 (first peak), #3 and #11. The dynamics of #6 and #9 are
5 particularly well represented by both models (Figure 6c). But these catchments have a very
6 shallow soil (Table 1) and are almost completely saturated on 09/08 at 12UTC, after only 6
7 hours of rainfall (see next section). Thus, the observed peaks are mainly explained by the
8 rainfall intensity peaks leading to saturation excess runoff. Both models well represent this
9 dynamic, showing that, for these small catchments (about 10 km²), water transfer was
10 satisfactorily represented.

11 As also shown by the global sensitivity analysis, for the different catchments, the simulated
12 peak hours by both models are quite similar although the transfer modules are different.
13 However, the amplitude of the peaks is much higher in CVN than in MARINE. Generally, the
14 sensitivity of MARINE to the Manning roughness coefficient is smaller than that of CVN.
15 This is likely because of channel flow modelling which accounts for drainage network within
16 floodplains. More detailed information about the river bed, such as its geometry and
17 roughness would help improve the transfer modules of both models. The availability of
18 distributed water height series (and preferably discharge series) at various scales could also be
19 helpful in better characterizing flow dynamics.

20

21 Table 3 also provides the runoff coefficient, RC, simulated by both models. The average
22 difference between MARINE and CVN RC estimation is 0.04 in the range [-0.01, 0.15] and
23 the root mean square difference is 0.07. The difference between both models in terms of
24 runoff coefficient is thus much higher than expected given the relative proximity in their
25 process representation. These differences in hydrological response also appear in Figure 10

1 which shows the relationships between the simulated RC and rainfall total amount, average
2 soil depth, initial storage deficit and initial saturation. On this graph, we have distinguished
3 between points with an acceptable or a bad simulation of maximum peak discharge. Figure 10
4 shows no significant correlation with all the variables for MARINE ($R^2 < 0.20$), whereas a
5 significant relationship is found between CVN RC and average soil depth ($R^2 = 0.62$, $p < 10^{-6}$,
6 Figure 10b) and initial soil water deficit ($R^2 = 0.75$, $p < 10^{-6}$, Figure 10c). These relationships
7 remain valid when only the “good” simulations are taken into account. In CVN, the strong
8 relationship between runoff generation, soil depth and initial storage deficit is expected as the
9 generated ponding is highly related to soil depth and/or water storage deficit in the case of full
10 saturation. As the ponding is directly routed to the river, all the ponding volume finally
11 reaches the outlet after being transferred within the river. The larger scatter for MARINE
12 could be explained by the hillslope routing which allows some re-infiltration before the water
13 reaches the river.

14 *Soil saturation dynamics*

15 Figure 11 maps the saturation state of each catchment at several times (from top to bottom: 8
16 September 2002 at 12hUTC, 9 September 2002 at 00hUTC, 9 September 2002 at 12hUTC).
17 The spatial distribution of the saturation states is quite similar for both models; however CVN
18 simulation results in higher saturation, as can be seen in Figure 12. The final saturation is 0.96
19 for CVN while it is 0.90 for MARINE. This difference may be related to CVN’s description
20 of the vertical soil heterogeneity as explained in the model set up section. MARINE exhibits
21 lower values of initial soil water storage deficit for deeper soils (Figure 4). However, the
22 saturated hydraulic conductivity used in MARINE is generally lower than the one used by
23 CVN with a ratio between both models ranging between 0.25 and about 9 (not shown). This
24 may explain both the lower final saturation and the higher RC obtained with MARINE. Table
25 2 shows that MARINE runoff coefficients are lower than CVN RC only for 2 catchments.

1 To illustrate the role of soil properties on the soil saturation dynamics, the mean saturation
2 state is plotted against different soil characteristics: soil classes (Figure 13a) and soil depths
3 (Figure 13b). Results show that soil spatial variability has a great impact on this dynamic.
4 Indeed, for both models, soils presenting high hydraulic conductivities (13.2 mm h^{-1} for class
5 n°4) or low depths (ranging between 0 m and 0.2 m) are rapidly saturated. The important
6 increase of saturation between September 8th 2002 at 18hUTC and September 9 at 00hUTC
7 can be explained by the accumulated rainfall during these 6h : locally more than 200 mm on
8 catchments presenting class 4 soil texture (#12, #6), and locally more than 150 mm on
9 catchments presenting low soil depths (#9, #11). For these soils, CVN and MARINE exhibit
10 almost the same saturation dynamics: the vertical soil heterogeneity is indeed of little
11 importance in these cases. CVN presents higher saturation states than MARINE for soils with
12 low hydraulic conductivities (0.6 mm h^{-1} for class n°11) or large depths (ranging between 0.8
13 m and 1 m) where soil can present high vertical heterogeneity. The important difference found
14 for soil class n°11 may also be explained by the soil parameter specifications of each model:
15 soil class n°11 covers an important range of soil textures (with a clay content ranging from 40
16 to 60%) with different values of soil parameters in CVN as continuous pedo-transfer
17 functions are used, while soil parameters are fixed for each soil class in MARINE. Indeed, it
18 can be seen in Figure 14b that the time evolution of the mean saturation states is highly
19 related to the soil class and therefore to hydraulic conductivity in MARINE, whereas it is
20 more related to soil depth (Figure 14a) in CVN. All these results emphasize the impact of the
21 spatial distribution of rainfall and soil properties on simulated soil saturation dynamics.

22 Figure 15 shows typical infiltration dynamics as simulated by the CVN models for different
23 soil STUs. Figure 15 shows that for the shallowest soils, full saturation is reached on 09/08 at
24 12hUTC on US 430 (Figure 15a) and US 425 (Figure 15c), with the generation of infiltration
25 excess runoff related to a low saturated hydraulic conductivity ($K_s=0.7 \text{ mm hr}^{-1}$). Even if

1 shallow, US 535 is saturated later on 09/09 at 00hUTC (Figure 15b) due to a higher $K_s=14$
2 mm hr^{-1} . These three soils are fully saturated on 09/09 at 00hUTC, leading to saturation
3 excess runoff until the end of the event. With the no flux boundary condition, these profiles
4 do not change until the end of the simulation within the CVN model. For US 528, a moderate
5 value of $K_s=4 \text{ mm hr}^{-1}$, and a deep soil lead to a topsoil saturation, and the generation of
6 infiltration excess runoff, on 09/09 at 00hUTC (Figure 15d), but infiltration can continue into
7 deeper layers until 09/09 at 12hUTC when the soil is fully saturated, generating saturation
8 excess runoff. Finally US 529 has a low $K_s=0.7 \text{ mm hr}^{-1}$ and two horizons. The first horizon is
9 saturated on 09/09 at 18hUTC, but infiltration continues into the second horizon (Figure 15e).
10 Infiltration excess runoff is generated throughout the whole event, but at the end, the soil is
11 not fully saturated and saturation excess runoff has not occurred in this soil. If US 529 is
12 assumed vertically homogeneous (Figure 15f), the topsoil saturation occurs later than with
13 the two horizons on 09/09 06hUTC, and the soil is not fully saturated at the end of the event.

14

15 *Impact of soil description on the simulated hydrographs*

16 Sensitivity tests exploring the impact of soil spatial variability on the CVN simulated
17 response are presented in this section for three catchments: #15, #17 and #18. Catchment #15
18 and #17 were chosen for this sensitivity study because they have a large variability of soils
19 with different storage capacity (Figure 4a) and hydraulic conductivities.

20 Simulations are performed using the same initial saturation rate as those given in Table 1.
21 Additional simulations are performed by using the same initial water storage deficit. Results
22 are shown in Figure 16a, b and c and Table 5. The impact on peak discharge is moderate (\pm
23 7% for #15 and #17 and +13% for #18), but the impact on runoff is significant with a
24 variation of ± 0.10 in the runoff coefficient. In general the changes in runoff are related to the
25 changes in initial soil water deficit and the increase/decrease in runoff amounts is equal to the

1 increase/decrease in initial storage deficit. When the same initial storage deficit is used for
2 initial conditions, runoffs are very similar, but there is an impact on peak discharge of $\pm 7\%$.
3 When soils are assumed to be vertically homogeneous instead of taking into account the
4 various horizons, the impact is limited to variations in the runoff coefficient and peak
5 discharge of a few percent. As does the previous analysis of soil saturation dynamics, this
6 sensitivity study highlights the importance of the initial water storage deficit on the
7 hydrological response at the outlet. Note that the quantification of initial conditions using a
8 saturation degree can lead to large differences in initial water storage deficit and is thus not
9 recommended. However, quantifying the initial soil water deficit is much more demanding in
10 terms of landscape description as it requires an accurate documentation of soil depths and
11 porosity.

12 *Impact of including subsurface flow within MARINE*

13 In order to test the impact of subsurface lateral flow within the MARINE model, a simulation
14 is performed with the same parameters as the reference simulation and activation of
15 subsurface lateral flow at a uniform subsurface velocity of 2 m.h^{-1} . This value is chosen as 50
16 times the averaged Green and Ampt hydraulic conductivity over the whole studied area.
17 Results show little sensitivity of peak discharge and runoff coefficient to subsurface flow with
18 a maximum difference of respectively -1% and $+0.03$ for #18 catchment. No impact on peak
19 time is observed. It seems that for such an extremely intense and short event, slow subsurface
20 lateral flow is of little importance in simulating peak time and discharge: with a simulation
21 duration of 30h and a subsurface velocity of 2 m.h^{-1} , no significant contribution of subsurface
22 flow to outlet hydrographs is simulated. This conclusion should however not be generalized to
23 less intense events. Indeed, introduction of subsurface flow slightly modifies the recession
24 simulation ($6 \text{ m}^3 \text{ s}^{-1}$ difference, hardly visible in Figure 16d), which may be of importance for
25 longer events with several rainfall peaks for instance. Moreover, the inclusion of subsurface

1 lateral flow has an important impact on distributed saturation dynamics. Indeed, Figure 17
2 maps the saturation state of catchment #18 at the end of the simulation (September 9th 2002 at
3 12hUTC) with and without subsurface flow. It clearly shows the importance of the drainage
4 network in the evolution of the saturation state when subsurface flow is considered. This is
5 due to the exfiltration that can occur in the drainage network. Measures describing the spatial
6 distributions of saturation state would be valuable to chose which processes must be
7 accounted for in the model.

8 **Discussion**

9 In this study, two distributed hydrological models are set up at the regional scale using the
10 available information and expert knowledge, without specific calibration. They are run for the
11 September 8-9 2002 event in the Gard on 18 sub-catchments ranging from 2.5 to 99 km²
12 where data of maximum peak discharge, and sometimes time of peak are available. Post flood
13 estimates of maximum peak discharge and time of peak are used to evaluate the models at the
14 regional scale. This kind of information is very valuable because it is the only information
15 available for small catchments. Up to now few studies (e.g. Bonnifait et al., 2009; Saulnier
16 and Le Lay, 2009) have targeted the regional scale in the study area. These studies were based
17 on a calibrated Topmodel approach. Bonnifait et al. (2009) also used the post flood field data
18 for model evaluation but the comparison was restricted to catchments larger than 50 km². The
19 originality of our study is to tackle very small catchments, which were shown to be the most
20 vulnerable to flash floods (Ruin et al., 2008).

21 The comparison between field estimates and simulated peak discharge shows a reasonable
22 agreement for half of the catchments for both models. The global sensitivity analysis on three
23 soil parameters and the Manning coefficient shows that the results of the reference simulation
24 in terms of maximum specific peak discharge are close to the median of the parameter set for
25 CVN and to the 25th quartile for MARINE. The uncertainty range of CVN are generally larger

1 than that of MARINE. Further analysis shows that CVN is more sensitive to the Manning
2 roughness coefficient of the river bed than MARINE (for which it is the floodplain roughness
3 coefficient) with a decrease of peak discharge when the Manning roughness coefficient is
4 increased. Peak discharge could be used to reduce the range of plausible Manning roughness
5 coefficients but, for the studied event, it seems difficult to find a unique value suitable for all
6 the catchments. For some catchments, the sensitivity study highlights probable problems with
7 the rainfall amount, as almost none of the parameter set is able to simulate the field peak
8 discharge. The time of peak is found quite stable with regards to the parameters and most of
9 the time, it is related to the time of high rainfall intensity peaks (larger than 100 mm hr^{-1}). The
10 CVN model is more sensitive to these peak intensities than the MARINE model. In CVN such
11 peak rainfall intensities generate infiltration excess runoff which is directly transferred to the
12 closest river reach, leading to large peak discharge. In MARINE, overland flow allows
13 possible re-infiltration of this infiltration excess runoff, and a smoothing of the impact of
14 those peaks. The corresponding peak discharge are therefore lower. Post flood estimates of
15 maximum discharge are therefore useful for analysing the impact of various flow routine
16 modules. However, they do not allow the evaluation of the simulated flow dynamics and the
17 identification of the most relevant model response. For this purpose, regional values of water
18 height (and possibly peak discharge) are required in order to base the analysis of the whole
19 hydrograph response. Our analysis should also be complemented by a study of the impact of
20 river geometry on the results.

21
22 In terms of runoff coefficient, post flood maximum discharge estimate do not provide a mean
23 to assess the relevance of the simulated results nor to discriminate between the two model
24 structures. The global and local sensitivity analysis highlight the large impact of soil depth,
25 saturated hydraulic conductivity and initial soil moisture on the simulated response, especially

1 in terms of runoff coefficient. The global sensitivity analysis also shows that several
2 combinations of these parameters can lead to similar responses in terms of peak discharge or
3 runoff coefficient. A better knowledge – at the regional scale- of soil depths, hydraulic
4 properties and initial conditions is therefore required in order to reduce uncertainty in these
5 parameters and in model results (Loague and VanderKwaak, 2004; Ebel and Loague, 2006).
6 For the extreme September 2002 event, very high runoff coefficient are simulated by both
7 models. Differences in model responses, related to the different model representation can be
8 highlighted but they are masked by the importance of the event.

9
10 In the present study, evapotranspiration and interception processes are neglected. This
11 hypothesis is reasonable given the duration of the event (one to two days) and the high rainfall
12 intensities during the event. Vegetation and land use is considered within MARINE for the
13 specification of the Manning roughness coefficient for overland flow, but a previous
14 sensitivity analysis showed that this parameter is not very influential (Le, 2008). On the other
15 hand, vegetation and land use do have a significant impact on initial conditions. A more
16 comprehensive version of the CVN model is under construction. It will be used to study the
17 impact of soil moisture. A continuous model is considered and an evapotranspiration module
18 is being added to the current version of the model with parameters depending on the land use
19 and vegetation.

20
21 Several studies (e.g., Carpenter and Georgakakos, 2004; Teztlaff and Uhlenbrook, 2005;
22 Chancibault et al., 2006; Cole and Moore, 2008; Saulnier and Le Lay, 2009) highlight the
23 importance of an accurate quantification of the rainfall spatio-temporal dynamics for an
24 accurate simulation of the catchment's response. This point is not explicitly addressed in our
25 study. However, some of our results about time of peak show the importance of high rainfall

1 intensity peaks on the modelled results. The highest sensitivity of the CVN model to those
2 rainfall peaks is certainly related to its very simple overland flow representation. This
3 component of the model can be improved in the future. For some catchments where problems
4 are encountered with both models, rainfall accuracy is questioned. Therefore, the study
5 confirms the need for further work on the improvement of high spatial and temporal rainfall
6 resolution, and on the appropriate location of rainfall with regards to catchments boundaries.
7 Although the September 2002 event is perhaps too extreme to fully illustrate this point – due
8 to a generalized soil saturation- our study also highlights the importance of the representation
9 of soil spatial variability, both in terms of soil depths, porosity and hydraulic properties.
10 Although infiltration excess runoff is generated for all the catchments due to the high rainfall
11 intensities, the soil water storage deficit is found to be very important when it comes to the
12 timing of the response. This is in particular related to the threshold effect of full saturation of
13 the soils. As a consequence, information about the initial soil water deficit is more relevant
14 for the characterization of the initial moisture conditions than is the saturation degree of the
15 catchments, as provided by the SAFRAN-ISBA-MODCOU model. However, the former
16 estimation requires more data than the latter, as soil depths and porosity must be known with
17 good accuracy. When subsurface lateral flow is considered, its impact on such an extreme
18 event is found to be negligible in terms of peak discharge and runoff volume. However this
19 conclusion must not be generalised to less intense events.
20 The saturation dynamics analysed at the regional scale, provide interesting insight into
21 hydrological processes. When subsurface flow is not activated, the soil saturation patterns are
22 mostly related to soil depth (and rainfall), whereas, when subsurface flow is considered, a
23 second pattern of organisation along the river network is observed. Such patterns are typical
24 of models based on the Topmodel concepts (e.g. Quinn et al., 1998). Patterns of soil moisture
25 have been reported for small catchments using in situ data (e.g. Western et al., 2004; Latron

1 and Gallart, 2007), but a much larger coverage would be required to assess the relevance of
2 our simulated patterns and the methodology proposed by Beldring et al. (1999) could be used.
3 Remote sensing of soil moisture has proven useful in reducing model parameter uncertainty in
4 hydrological models (e.g. Franks et al., 1998) and has been shown to improve their
5 performance (e.g. Pauwels et al., 2001). However, remote sensing only provides retrieval of
6 topsoil moisture whereas an integrated value over the whole profiles would be required.
7 Works are conducted to retrieve integrated soil moisture over the root zone from the
8 combination of surface soil moisture and soil vegetation atmosphere transfer modelling (e.g.
9 Calvet and Noilhan, 2000; Montaldo et al., 2003; Albergel et al., 2008). The application of
10 such techniques on the studied region should be evaluated, because information about
11 integrated soil moisture content is required to assess which of our simulated patterns is the
12 most realistic.

13 The general methodology proposed in this paper is the following i) set up of distributed
14 hydrological models at the regional scale using the available data and expert knowledge
15 without specific calibration; ii) a regional evaluation using the available information such as
16 available hydrographs, post flood data of maximum peak discharge and time of peak; iii)
17 sensitivity studies to input data, parameters and process representation in order to get insight
18 into the most sensitive points and derive information about processes, data and parameters
19 requiring further measurements and understanding. It is applied to the September 2002
20 extreme event where the required data is available. Some interesting conclusions, summarized
21 below are drawn from this study. However, the event is so extreme that a general saturation of
22 the catchment is simulated, and the impact of various modelling hypotheses cannot be fully
23 examined. The study should be repeated with less extreme events (Merz and Plate, 1997) in
24 order to get more contrasted responses between catchments and models. The methodology
25 can also be applied to other regions, provided the required data are available.

1

2 **Conclusions**

3 In the introduction, four questions are highlighted. The results presented in this paper provide
4 some interesting responses. The study shows that it is possible to set up , at the regional scale,
5 distributed hydrological models, relevant for flash flood simulation, using available data and
6 expert knowledge. It is a step towards the “model of everywhere”, advocated by Beven
7 (2003). Provided high spatial and temporal resolution of rainfall is available, post flood field
8 data of maximum peak discharges and time of peak are valuable for the regional evaluation of
9 these models. However, they are not sufficient for a full assessment of the simulated
10 hydrological response in terms of flow dynamics, runoff coefficient and soil saturation
11 dynamics. Model sensitivity studies including input data, parameters and process
12 representation are very valuable in order to highlight where additional data could be useful.

13

14 This point is further detailed below where an experimental set up, suitable for improved
15 understanding and modelling of flash floods is proposed in the context of the future HyMeX
16 program. This experimental set up is based on nested instrumented catchments at various
17 scales: i) densely instrumented small catchments of 1-10 km², where process studies can be
18 conducted; ii) larger instrumented catchments (of about 100-500 km²) where the change of
19 scale problem can be tackled and, iii) regional catchments (of about 1000-10000 km²), where
20 operational data are collected. Such a strategy is already implemented in African within the
21 AMMA project (Lebel et al., 2009), or in the UK in the framework of the Catchment
22 Hydrology And Sustainable Management program (O’Connell et al., 2007). For flash floods
23 studies, the following recommendations can be made:

- 24 • The information provided by post event field experiments about maximum peak discharge
25 and time of peak is definitively recognised as very valuable, especially for small

1 catchments. But the availability of enhanced networks of discharge series and/or water
2 levels would increase our capability to specify hydrological models parameters and
3 improve the process representations, through a better knowledge of the flow dynamics.
4 The set up of LS-PIV (Large Scale Particle Image Velocimetry) networks (Muste et al.,
5 2005; Le Coz et al., 2009²) and/or water level measurement networks (Sarrazin et al.,
6 2009) which increase the density of this information in nested catchments is therefore
7 encouraged.

- 8 • The spatial variability of soil depth and soil porosity, as well as hydraulic properties is
9 found to be influential on the hydrological response and more specifically on the soil
10 saturation patterns and dynamics. Up to now, this variability has been described through
11 pedological maps, which are built for agronomic purposes, but not necessarily relevant to
12 hydrological purposes since we are interested in the whole soil profiles, including the
13 potentially altered substratum. The description of soil properties such as soil depth,
14 porosity and hydraulic conductivity should thus be enhanced at the regional scale.
- 15 • Finally this study proposes different patterns of soil saturation dynamics according to
16 different model hypotheses about the role of subsurface lateral flow. Regional mapping of
17 soil saturation, over the whole profiles, would be required to determine which patterns are
18 the most realistic as compared to field conditions. A combination of remote sensing data,
19 in situ local measurements, and data assimilation could provide the necessary data.

20 **Acknowledgments**

21 The work presented in this paper was partly funded by the HYDRATE European Commission
22 FP6 project under the n°GOCE 37024. Olivier Vannier is thanked for processing the witness
23 interviews used in the study. Radar data and part of the rainfall data were provided by Météo-

² Le Coz, J., Hauet, A., Dramais, G., Pierrefeu, G., 2010. Improvement of flash-flood discharge measurements using image-based velocimetry (LS-PIV), Journal of Hydrology, Flash Floods special issue, accepted.

1 France. We acknowledge Electricité de France and the flood forecasting service SPC-GD for
2 the availability of the discharge data and the rest of rainfall data. The ST-AD3 radar data were
3 provided by Brice Boudevillain from LTHE Grenoble. Two anonymous reviewers and the
4 editors helped improving the quality of the paper. Stéphanie Moore carefully checked the
5 English language.

6 **References**

- 7
- 8 Albergel, c., Rüdiger, C., Pellarin, T., Calvet, J.C., Fritz, N., Froissard, F., Suquia, D., Petitba,
9 A., Piguet, B. and Martin, E., 2008. From near-surface to root-zone soil moisture using an
10 exponential filter: an assessment of the method based on in-situ observations and model
11 simulations. *Hydrology and Earth System Sciences Discussion*, 12, 1323-1337.
- 12 Beldring, S., Gottschalk, L., Seibert, J., Tallaksen, L.M., 1999. Distribution of soil moisture
13 and groundwater levels at patch and catchment scales. *Agricultural and Forest Meteorology*,
14 98-99, 305-324.
- 15 Bessière, H., 2008. Assimilation de données variationnelle pour la modélisation hydrologique
16 distribuée des crues à cinétique rapide. Thèse de doctorat, Institut National Polytechnique
17 de Toulouse, Toulouse, France, 350 pp.
- 18 Bessière, H., Roux, H., Dartus, D., 2008. Data assimilation for distributed flash flood
19 modelling. *Proceedings of the International Symposium on "Weather Radar and*
20 *Hydrology"*, WRaH2008, March 10-12 2008, Grenoble, France, 4pp.
- 21 Beven, K., 2003. On environmental models of everywhere on the GRID. *Hydrological*
22 *Processes*, 17, 171-174.
- 23 Beven, K., Kirkby, M. J., 1979. A physically-based variable contributing area model of basin
24 hydrology, *Hydrological Sciences Bulletin*, 24, 43-69.

- 1 Bonnifait, L., Delrieu, G., Le Lay, M., Boudevillain, B., Masson, A., Belleudy, P., Gaume, E.,
2 Saulnier, G.M., 2009. Distributed hydrologic and hydraulic modelling with radar rainfall
3 input: Reconstruction of the 8–9 September 2002 catastrophic flood event in the Gard
4 region, France, *Advances in Water Resources*, 37(7), 1077-1089.
- 5 Borga, M., Gaume, E., Creutin, J.D., Marchi, L., 2008. Surveying flash floods: gauging the
6 ungauged extremes. *Hydrological Processes*, 22, 3883-3885.
- 7 Brooks R.H., Corey, A.T., 1964. Hydraulic properties of porous media. *Hydrology Papers*,
8 Colorado State University, 24 pp.
- 9 Calvet, J.C., Noilhan, J., 2000. From near-surface to root zone soil moisture using year-round
10 data. *Journal of Hydrometeorology*, 1(5), 393-411.
- 11 Carpenter, T.M. and Georgakakos, K.P., 2004. Impacts of parametric and radar rainfall
12 uncertainty on the ensemble streamflow simulations of a distributed hydrologic model, *J. of*
13 *Hydrology*, 299, 202-221.
- 14 Chancibault, K., S. Anquetin, V. Ducrocq, and G. M. Saulnier, 2006. Hydrological evaluation
15 of high-resolution precipitation forecasts of the Gard flash-flood event (8-9 September
16 2002). *Q. J. R. Meteo. Soc.*, 132, 1091-1117.
- 17 Cole, S.J. and Moore, R.J., 2008. Hydrological modelling 1 using raingauge- and radar based
18 estimators of areal rainfall, *J. of Hydrology*, 358, 159-181.
- 19 Crevoisier, D., Chanzy, A., Voltz, M., 2009. Evaluation of the Ross fast solution of Richards'
20 equation in unfavourable conditions for standard finite element methods. *Advances in*
21 *Water Resources*, 32(6), 936-947.
- 22 Dehotin, J., Braud, I., 2008, Which spatial discretization for distributed hydrological models?
23 Proposition of a methodology and illustration for medium to large-scale catchments,
24 *Hydrol. Earth Sys. Sci.*, 12, 769-796.

- 1 Delrieu G., Ducrocq, V., Gaume, E., Nicol, J., Payrastre, O., Yates, O., Kirstetter, P.E.,
2 Andrieu, H., Ayrat, P.-A., Bouvier, C., Creutin, J.-D., Livet, M., Anquetin, S., Lang, M.,
3 Neppel, L., Obled, C., Parent-du-Châtelet, J., Saulnier, G.-M., Walpersdorf, A., Wobrock,
4 W. 2005, The catastrophic flash-flood event of 8-9 September 2002 in the Gard region,
5 France: a first case study for the Cévennes-Vivarais Mediterranean Hydro-meteorological
6 Observatory, *J. Hydrometeorology*, 6, 34-52.
- 7 Delrieu, G., Boudevillain, B., Nicol, J., Chapon, B., Kirstetter, P.E., Andrieu, H., Faure, D.,
8 2009, Bollène 2002 experiment: radar rainfall estimation in the Cevennes-Vivarais region.
9 *Journal of Applied Meteorology and Climatology*: DOI: 10.1175/2008JAMC1987.1.
- 10 Drobinski, P., Ducrocq, V., (Coordination), Béranger, K., Braud, I., Carlotti, F., Claud, C.,
11 Delrieu, G., Doerenbecher, A., Despiau, S., Dulac, F., Durrieu de Madron, X., Elbaz, F.,
12 Escadafal, R., Estournel, C., Gordani, H., Guieu, C., Guiot, J., Hallegate, S., Kageyama, M.,
13 Jacob, F., Lachassagne, P., Li, L., Martin, E., Médail, F., Noilhan, J., Moussa, R., Perrin,
14 J.L., Plu, M., Pireur, L., Ricard, D., Rinaudo, J.C., Roux, F., Somot, E., Taupier-Lepage, I.,
15 HyMeX : Towards a major field experiment in 2010-2020. White book. Draft 1.3.2,
16 February 2008. 124 pp.
17 http://www.cnrm.meteo.fr/hymex/index.php?lang=english&page=main_documents
- 18 Ebel, B.A., Loague, K., 2006. Physics-based hydrologic response simulation: seeing through
19 the fog of equifinality. *Hydrological Processes*, 20, 2887-2900.
- 20 Franks, S.W., Gineste, P., Beven, K.J., Merot, P., 1998. On constraining the predictions of a
21 distributed model: the incorporation of fuzzy estimates of saturated areas into the calibration
22 process. *Water Resources Research*, 34(4), 787-797.
- 23 Gaume, E., Bain, V., Bernardara, P., Newinger, O., Barbuc, M., Bateman, A., Blaskovicová,
24 L., Blöschl, G., Borga, M., Dumitrescu, A., Daliakopoulos, I., Garcia, J., Irimescu, A.,
25 Kohnova, S., Koutroulis, A., Marchi, L., Matreata, S., Medina, V., Preciso, E., Sempere-

- 1 Torres, D., Stancalie, G., Szolgay, J., Tsanis, I., Velasco, D. and Viglione, A., 2009. A
2 compilation of data on European flash floods. *Journal of Hydrology*, 367(1-2), 70-78.
- 3 Gaume, E., Bouvier, E., 2004, Analyse hydro-pluviométrique des crues du Gard et du
4 Vidourle des 8 et 9 septembre 2002. *La Houille Blanche*, 6, 99-106. DOI :
5 10.1051/lhb:200406014
- 6 Georgakakos, K. P., 2006, Analytical results for operational flash flood guidance. *J. Hydrol.*,
7 317(1–2), 81–103, doi:10.1016 / j.jhydrol.2005.05.009.
- 8 Green, W.H., Ampt, G.A. 1911. Studies in soil physics: I. The flow of air and water through
9 soils. *J. Agric. Sci.*, 4,1-24.
- 10 Habets, F., Boone, A., Champeaux, J.L., Etchevers, P., Franchistéguy, L., Leblois, E.,
11 Ledoux, E., Le Moigne, P., Martin, E., Morel, S., Noilhan, J., Quintana-Segui, P., Rousset-
12 Regimbeau, F., Viennot, P., 2008. The SAFRAN-ISBA-MODCOU hydrometeorological
13 model applied over France. *Journal of Geophysical Research*, 113, D06113,
14 doi:10.1029/2007JD008548.
- 15 Kampf, S.K., Burges, S.J., 2007. A framework for classifying and comparing distributed
16 hillslope and catchment hydrologic models. *Water Resources Research*, 43, W05423,doi:
17 10.1029/2006WR005370.
- 18 Ivanov, V.Y., Vivoni, E.R., Bras, R.L., Entekhabi, D., 2004. Catchment hydrologic response
19 with a fully distributed triangulated irregular network model. *Water Resources Research*,
20 40(11), W11102, doi: 10.1029/2004WR003218.
- 21 Latron, J., Gallart, F., 2007. Seasonal dynamics of runoff-contributing areas in a small
22 mediterranean research catchment (Vallcebre, Eastern Pyrenees). *Journal of Hydrology*,
23 335(1-2), 194-206.

- 1 Le, X.K., 2008. Variabilité des processus hydrologiques entrant dans le mécanisme de la
2 genèse des crues sur les bassins à cinétique rapide. Thèse de doctorat, Institut National
3 Polytechnique de Toulouse, Toulouse, France, 147 pp.
- 4 Lebel, T., Cappelaere, B., Galle, S., Hanan, N., Kergoat, L., Levis, S., Vieux, B., Descroix,
5 L., Gosset, M., Mougou, E., Peugeot, C., Seguis, L., 2009. AMMA-CATCH studies in the
6 Sahelian region of West-Africa: An overview. *Journal of Hydrology*, 375(1-2), 3-13.
- 7 Liu, Z., Todini, E., 2002. Towards a comprehensive physically-based rainfall-runoff model.
8 *Hydrology and Earth System Sciences*, 6(5), 859-881.
- 9 Loague, K., Heppner, C., Mirus, B.B., Ebel, B.A., Carr, A.E., DBeVill, S.H., VanderKwaak,
10 J.E., 2006. Physics-based hydrologic response simulation: foundation for hydroecology and
11 hydrogeomorphology. *Hydrological Processes*, 20, 231-1237.
- 12 Loague, K., VanderKwaak, J.E., 2004. Physics-based hydrologic response simulation:
13 platinum bridge, 1958 Edsal, or useful tool. *Hydrological Processes*, 18, 2949-2956.
- 14 Manus, C., Anquetin, S., Braud, I., Vandervaere, J.P., Viallet, P., Creutin, J.D. and Gaume,
15 E., 2009. A modelling approach to assess the hydrological response of small Mediterranean
16 catchments to the variability of soil characteristics in a context of extreme events,
17 *Hydrology and Earth System Sciences*, 13, 79-97.
- 18 Merz, B., Plate, E.J., 1997. An analysis of the effects of spatial variability of soil and soil
19 moisture on runoff. *Water Resources Research*, 33(12), 2909-2922.
- 20 Montaldo, N., Albertson, J.D., 2003. Multi-scale assimilation of surface soil moisture data for
21 robust root zone moisture predictions. *Advances in Water Resources*, 26, 33-44.
- 22 Marchandise, A., 2007. Modélisation hydrologique distribuée sur le Gardon d'Anduze; étude
23 comparative de différents modèles pluie-débit, extrapolation de la normale à l'extrême et
24 tests d'hypothèses sur les processus hydrologiques, Université de Montpellier II,
25 Montpellier, 234 pp.

- 1 Maubourguet, M-M., Chorda, J., Dartus, D., George, J., 2007. MARINE : Prévission des crues
2 éclair sur le Gardon d'Anduze. 1st HyMeX workshop, 9-11 January 2007, Toulouse, France.
3 Short Abstracts B19, p.57
- 4 Muste, M., Schone, J., Creutin, J.D., 2005. Measurements of free-surface flow velocity using
5 controlled surface waves, Flow Measurement and instrumentation, 16(1), 47-55.
- 6 Norbiato, D., Borga, M., Esposti, S.D., Gaume, E. and Anquetin, S., 2008. Flash flood
7 warning based on rainfall thresholds and soil moisture conditions: An assessment for
8 gauged and ungauged basins. Journal of Hydrology, 362, 274-290.
- 9 Noto, L.V., Ivanov, V.Y., Bras, R.L., Vivoni, E.R., 2008. Effects of initialization on response
10 of a fully-distributed hydrologic model. Journal of Hydrology, 352(1-2), 107-125.
- 11 O'Connell, E., Ewen, J., O'Donnell, G., Quinn, P.F., 2007. Is there a link between agricultural
12 land-use managemetn and flooding? Hydrology and Earth System Sciences, 11(1), 96-107.
- 13 Piñol, J., Beven, K.J., Freer, J., 1997. Modelling the hydrologocal response of mediterranean
14 catchments, Prades, Catalonia. The use of distributed models as aids to hypothesis
15 formulation. Hydrological Processes, 11, 1287-1306.
- 16 Pauwels, V.R.N., Hoeben, R., Verhoest, N.E.C., De Troch, F.P., 2001. The importance of the
17 spatial patterns of remotely sensed soil moisture in the improvement of discharge
18 predictions for small-scale basins through data assimilation. Journal of Hydrology, 251, 88-
19 102.
- 20 Quinn, P.F., Ostendorf, B., Beven, K., Tenhunen, J., 1998. Spatial and temporal predictions
21 of soil moisture patterns and evaporative losses using TOPMODEL and the GAS-FLUX
22 model for an Alaskan catchment. Hydrology and Earth System Sciences, 2(1), 51-64.
- 23 Rawls, W.J., Brakensiek, D.L., 1983. A procedure to predict Green Ampt infiltration
24 parameters, Adv. Infiltration, Am. Soc. Agric. Eng., 102-112

- 1 Rawls W.J., Brakensiek, D.L., 1985, Prediction of soil water properties for hydrologic
2 modelling. Jones, E.B. and Ward, T.J. eds. Watershed management in the eighties:
3 proceedings of the American Society of Civil Engineers symposium, Denver, April 30-May
4 1,1985. ASCE, New York, 293-299.
- 5 Reed, S., Schaake, J., Zhang, Z., 2007, A distributed hydrologic model and threshold
6 frequency-based method for flash flood forecasting at ungauged locations. Journal of
7 Hydrology, Vol. 337, Issue 3-4, 402-420.
- 8 Refsgaard, J.C., 1997. Parameterisation, calibration and validation of distributed hydrological
9 models. J. of Hydrology, 198, 69-97
- 10 Ross, P.J., 2003, Modeling soil water and solute transport - Fast, simplified numerical
11 solutions. Agronomy Journal, 95, 1352-1361.
- 12 Ruin, I., Creutin, J.D., Anquetin, S., Lutoff, C., 2008. Human exposure to flash-floods-
13 relation between flood parameters and human vulnerability during a storm of September
14 2002 in Southern France. Journal of Hydrology, 361, 199-213.
- 15 Sangati, M., Borga, M., Rabuffeti, D., Bechini, R., 2009. Influence of rainfall and soil
16 properties spatial aggregation on extreme flash flood response modelling: an evaluation
17 based on the Sesia river basin, North Western Italy. Advances in Water Resources, 32,
18 1090-1106.
- 19 Sarrazin, B., Braud, I., Lagouy, M., Bailly, J.S., Puech, C., Ayroles, H., 2009. A distributed
20 water level network in ephemeral river reaches to identify the hydrological responses of
21 anthropogenic catchments, EGU General Assembly, 19-24 April 2009, Vienna, Austria,
22 *Geophysical Research Abstracts*, Vol 11, EGU2009-6103
- 23 Saulnier, G.M., Le Lay, M., 2009. Sensitivity of flash-flood simulations on the volume, the
24 intensity, and the localization of rainfall in the Cévennes-Vivarais region (France). Water
25 Resources Research, 45, W10425, doi: 10.1029/2008WR0069056.

- 1 Tarboton, D.G., 1997. A new method for the determination of flow directions and
2 contributing areas in Grid Digital Elevation models. *Water Resources Research*, 33(2), 309-
3 319.
- 4 Tetzlaff, D. and Uhlenbrook, S., 2005. Significance of spatial variability in precipitation for
5 process-oriented modelling: results from two nested catchments using radar and ground
6 station data. *Hydrol. Earth Sys. Sci.*, 9: 29-41.
- 7 van Griensven, A., Meixner, T., Grunwald, S., Bishop, T., Diluzio, M., Srinivasan, R., 2006.
8 A global sensitivity analysis tool for the parameters of multi-variable catchment models.
9 *Journal of Hydrology*, 324(1-4), 10-23.
- 10 Varado, N., Ross, P.J., Braud, I., Haverkamp, R., 2006, Assessment of an efficient numerical
11 solution of the Richards' equation for bare soil. *J of Hydrol.*, 323(1-4), 244-257.
- 12 Viallet, P., Debionne, S., Braud, I., Dehotin, J., Haverkamp, R., Saâdi, Z., Anquetin, S.,
13 Branger, F., Varado, N., 2006, Towards multi-scale integrated hydrological models using
14 the LIQUID framework, 7th International Conference on Hydroinformatics 2006, 4-8
15 September, Nice, France, Vol I, pp. 542-549.
- 16 Vivoni, E.R., Entekhabi, D., Bras, R.L., Ivanov, V.Y., 2007. Controls on runoff generation
17 and scale-dependence in a distributed hydrological model. *Hydrology and Earth System*
18 *Sciences*, 11, 1683-1701.
- 19 Western, A.W., Zhou, S.L., Grayson, R.B., McMahon, T.A., Blöschl, G., Wilson, D.J., 2004.
20 Spatial correlation of soil moisture in small catchments and its relationship to dominant
21 spatial hydrological processes. *Journal of Hydrology*, 286(1-4), 113-134.
- 22 Younis, J., Anquetin, S., Thielen, J., 2008, The benefit of High-Resolution operational
23 weather forecasts for flash-flood warning, *Hydrology and Earth System Sciences* 12, 1039-
24 1051.

List of figures

Figure 1. Location of the study area, location of the simulated catchments and slope map of the region. The catchment numbers are those of Table 1. Coordinates are in extended Lambert II (m)

Figure 2. Scheme of the MARINE model. a) MARINE model structure. b) Geometry of a network cross section within the MARINE model

Figure 3. Scheme of the CVN model. Step 1 derives the hydrographic network and sub-catchments boundary from the DTM. The river network provides the geometry for the 1D flow routine module. Step 2 derives the hydro-landscapes, used as elementary modeling unit for the Richards equation infiltration module, from the overlay of the pedology map and sub-catchments boundaries. The hydro-landscapes are sub-divided into layers to account for soil vertical heterogeneity and ponding is directly transferred to the closest river reach.

Figure 4. a) Maximum soil water storage capacity (mm) for the studied catchments. b) Total cumulated rainfall (mm) between 2002/09/08 06hUTC and 2002/09/09 12hUTC. c) Initial soil water deficit (mm) for the CVN model on 2002/09/08 06hUTC. d) Initial soil water deficit (mm) for the MARINE model on 2002/09/08 06hUTC.

Figure 5. a) Comparison of simulated (● for CVN and ▲ for MARINE) and field estimation of maximum peak discharge in a log-scale. The vertical bars along the 1:1 lines correspond to the uncertainty in the estimated values. b) Comparison of simulated (● for CVN and ▲ for MARINE) and field estimation (□ with the corresponding error bar) maximum specific peak discharge. The x-axis provides the catchment numbers (see Table 1) and the catchments are ordered with increasing area.

Figure 6. Boxplot of the global sensitivity analysis results on maximum specific peak discharge (top) and runoff coefficient (bottom) for the CVN model (left) and MARINE model (right). The thick line in the boxplot represents the median, the limits of the box provide the

25th and 75th quartiles and the whiskers provide the 95% confidence interval. Crosses are the outliers. For maximum specific discharge, the black points with the thick vertical lines are the *in situ* field estimates with their uncertainty range (see Table 3), and the black squares are the results of the reference simulation.

Figure 7. Most significant results of the sensitivity analysis for catchment #15 (grabieux). (a) Maximum specific discharge as a function of Manning roughness coefficient ($m^{-1/3}$ s). The horizontal full line is the *in situ* field estimate with its uncertainty (dashed line). Runoff coefficient as function of the (b) multiplicative factor for saturated hydraulic conductivity; (c) soil depth; and (d) of initial soil moisture. CVN results appear as black squares and MARINE results as open triangles. The larger symbols correspond to the reference simulation.

Figure 8. Examples of simulated hydrographs by the MARINE and CVN models for catchments (a) #1, (b) #3, (c) #9, (d) #15, (e) #17, (f) #18. The horizontal full lines are the field estimated peak discharge and the horizontal dashed lines are the confidence intervals. Crosses are drawn at the time of peaks as retrieved from witness interviews. The observed hydrograph for catchment #18 is shown with black squares on panel (f). Catchments are presented in the figure in increasing area order.

Figure 9. Sensitivity study to the specification of the Manning coefficient of the CVN model (reference value: $n=0.05 m^{-1/3}$ s, tested value: $n=0.125 m^{-1/3}$ s) and of the floodplain Manning coefficient of the MARINE model (reference value: $n=0.125 m^{-1/3}$ s; tested value: $n=0.05 m^{-1/3}$ s) for (a) #10; (b) #15; (c) #17; (d) #18.

Figure 10. Relationship between catchment simulated runoff coefficients and (a) total rainfall amount; (b) average soil depth; (c) initial soil water deficit (mm); (d) initial saturation ratio. The graphs distinguished catchments for which the simulation of maximum peak discharge is within the error bounds (“good”) and out the error bounds (“bad”).

Figure 11. Maps of the simulated soil saturation state by CVN (left) and MARINE (right) for three dates: 09/08 12hUTC (top), 09/09 00hUTC (middle) and 09/09 12hUTC (bottom).

Figure 12. Time evolution of the average saturation state over the whole studied area for both models.

Figure 13. Example of time evolution of the mean saturation state for different types of soils a) Rawls and Brakensiek 4 and 11 soil classes (4: loam; 11: clay); Soil depths ranging between 0-0.2 m and 0.8-1 m are distinguished.

Figure 14. Correlation of the saturation dynamics with soil properties at several times (square: 8 september at 12:00; triangle: 9 september at 00h; diamond: 9 september at 12h) a) Soil depths for CVN; b) Soil classes for MARINE (4: loam; 7: clay loam; 11: clay - Only soil classes present in more than 1000 cells of the grid have been taken into account).

Figure 15. Time evolution of the soil saturation profiles of six different soils on different catchments. (a) #15 US 430; (b) #15 US 535; (c) #17 US 425; (d) #15 US 528; (e) #17 US 529; (f) #17 US 529 vertically homogeneous. The symbols correspond to the various dates: (full line) 2002/09/08 06h00; (■) 2002/09/08 12h00; (▲) 2002/09/08 18h00; (□) 2002/09/09 00h00; (■) 2002/09/09 12h00; (+) 2002/09/09 12h00.

Figure 16. (a) Sensitivity to the soil representation on #15 for the CVN model; (b) Sensitivity to the soil representation on #17 for the CVN model (c) Sensitivity to the soil representation on #18 for the CVN model; (d) Sensitivity of the MARINE model to inclusion of sub-surface flow on #18

Figure 17. Spatial distribution of the saturation state of #18 catchment on September 9 2002 at 12hUTC simulated with MARINE model a) without subsurface lateral flow b) with subsurface lateral flow at a uniform velocity of 2 m.h^{-1} .

Table 1. Characteristics summary of the studied catchments, ordered by increasing area.

#	Catchment name	Area (km ²)	Average soil depth (cm)	CVN maximum storage capacity (mm)	MARINE maximum storage capacity (mm)	Initial saturation (%)	CVN initial storage deficit (mm)	MARINE initial storage deficit (mm)
1	alzon_sec05	2.5	49	155	146	54	71	67
2	alzon_sec04	3.4	21	94	88	54	43	40
3	droude_sec04	4.0	84	374	352	55	169	158
4	braune_sec06	7.3	45	161	148	58	67	61
5	alzon_sec01	8.2	25	109	98	54	50	45
6	ourne_sec03	10.2	25	104	98	58	43	41
7	braune_sec05	11.6	43	145	137	57	62	59
8	bourdic_sec02	12.0	45	145	97	62	43	41
9	ourne_sec02	12.0	26	103	137	58	55	52
10	braune_sec01	14.6	73	223	208	58	92	86
11	alzon_sec03	16.0	30	123	113	54	56	52
12	crieulon_sec01	19.0	96	397	366	68	128	117
13	galeizon_sec05	21.0	18	62	59	48	33	31
14	braune_sec04	23.3	64	249	231	59	102	95
15	grabieux_sec02	24.1	45	185	168	56	80	73
16	galeizon_sec03	38.1	22	72	68	47	37	36
17	courme_sec04	50.2	81	336	314	61	131	123
18	saumane	99.0	19	68	53	46	36	29

Table 2: Distributions and range of the parameters used in the global sensitivity analysis

Parameter	Range	Type of distribution	Comment
Multiplicative factor for saturated hydraulic conductivity	[0.01, 100]	log-normal	Local in situ field measurements report high saturated hydraulic conductivity (Marchandise, 2007)
Multiplicative factor for soil depth	[0.01, 10]	Log-normal	
Manning coefficient (main channel for CVN, floodplain for MARINE)	[0.01, 0.2]	Log-normal	From the literature
Initial soil saturation	[0,1]	uniform	

Table 3. Estimated and simulated maximum peak discharge. Estimated and simulated time of peak. When two values are provided, it corresponds to two successive peaks. Simulated runoff coefficients (RC) for the MARINE and CVN models.

#	Estimated peak discharge (m ³ s ⁻¹) ¹⁾	Estimated time of peak (UT).	Total accumulated rainfall (mm)	CVN simulated peak discharge (m ³ s ⁻¹)	MARINE simulated peak discharge (m ³ s ⁻¹)	CVN simulated time of peak	MARINE simulated time of peak	CVN runoff coefficient	MARINE runoff coefficient
1	100 [80 - 125]	09/09 01:00-02:00 09/09 05:00-06:00	526	109	68	09/09 00:10 09/09 05:40	09/09 00:15 09/09 05:10	0.90	0.92
2	100 [70 - 120]	-	393	85	72	-	-	0.88	0.90
3	40 [30 - 50]	08/09 22:00 09/09 05:00-06:00	368	95	56	08/09 21:00 09/09 08:10	08/09 20:40 09/09 07:20	0.72	0.87
4	160 [120 - 200]	-	441	185	91	-	-	0.84	0.85
5	330 [270 - 370]	-	436	269	207	-	-	0.87	0.89
6	270 [220 - 350]	09/09 02:00 09/09 05:00	502	272	226	09/09 02:10 09/09 05:40	09/09 02:00 09/09 05:40	0.91	0.92
7	230 [170 - 290]	-	420	390	170	-	-	0.85	0.92
8	111 [100 - 111]	-	371	213	156	-	-	0.85	0.94
9	300 [250 - 350]	09/09 02:00 09/09 05:00	505	333	271	09/09 02:10 09/09 05:40	09/09 02:00 09/09 05:50	0.91	0.91
10	60 [40 -]	-	339	419	163	-	-	0.79	0.87
11	430 [300 - 550]	09/09 03:00-03:30	480	532	376	09/09 05:40	09/09 05:40	0.89	0.90
12	320 [285 - 380]	-	451	357	217	-	-	0.78	0.85
13	400 [320 - 490]	-	336	452	375	-	-	0.90	0.89
14	300 [200 - 400]	-	429	359	320	-	-	0.77	0.83
15	390 [310 - 470]	-	404	522	348	-	-	0.79	0.82
16	400 [350 - 500]	-	267	645	616	-	-	0.86	0.88
17	635 [590 - 730]	09/09 10:00	360	539	307	09/09 09:30	09/09 9:40	0.75	0.89
18	770 [650 - 1050]	09/09 05:00	207	1673	1175	09/09 04:30	09/09 04:20	0.84	0.83

Table 4. Sensitivity study to the specification of the Manning coefficient of the CVN model (reference value: $n=0.05 \text{ m}^{-1/3} \cdot \text{s}$, tested value: $n=0.125 \text{ m}^{-1/3} \cdot \text{s}$;) and of the floodplain Manning coefficient of the MARINE model (reference value: $n=0.125 \text{ m}^{-1/3} \cdot \text{s}$; tested value: $n=0.05 \text{ m}^{-1/3} \cdot \text{s}$;) for 4 catchments.

#	CVN peak discharge ($\text{m}^3 \text{ s}^{-1}$)	CVN time of peak (UTC)	CVN peak discharge ($\text{m}^3 \text{ s}^{-1}$)	CVN time of peak (UTC)	MARINE peak discharge ($\text{m}^3 \text{ s}^{-1}$)	MARINE time of peak (UTC)	MARINE peak discharge ($\text{m}^3 \text{ s}^{-1}$)	MARINE time of peak (UTC)
<i>n</i>	0.05		0.125		0.05		0.125	
3	95	09/08 21h00	65	09/08 21h10	71	09/08 20h40	65	09/08 21h10
15	516	09/09 05h50	375	09/09 05h50	435	09/09 05h40	348	09/09 06h10
17	539	09/09 09h30	345	09/09 10h20	446	09/09 09h00	307	08/09 21h30
18	1673	09/09 04h30	1392	09/09 05h00	1291	09/09 04h00	1175	09/09 04h20

Table 5. Sensitivity studies using the CVN model. The reference simulations were performed with the distributed soils and a Manning roughness coefficient of 0.05. US 528, 535, 607 belong to MARINE textural class 4 (loam); US 430 and 529 to class 7 (clay loam); and US 425 to class 11 (clay).

Simulation	Initial water storage deficit (mm)	Maximum peak discharge ($\text{m}^3 \text{s}^{-1}$)	Time of peak (UT) 2002/09/09	Total runoff (mm)	Runoff coefficient
Grabieux #15 (rainfall 404 mm)					
Reference simulation	80	522	05h40	323	0.80
Uniform soil US 430	30	548	05h40	372	0.92
Uniform soil US 528	134	486	05h40	269	0.66
Uniform soil US 535	64	548	05h40	338	0.84
Uniform soil US 528	80	548	05h40	320	0.79
Courme #17 (rainfall 359 mm)					
Reference simulation	131	539	09h30	271	0.75
Uniform soil US 528	123	570	09h20	232	0.64
Uniform soil US 529	172	514	09h30	255	0.71
Uniform soil US 430	52	573	09h20	299	0.83
Uniform soil US 529	131	514	09h30	255	0.71
Uniform soil US 529 vertically homogeneous	166	513	09h30	247	0.69
Saumane #18 (rainfall 208 mm)					
Observation	-	770	06h00	85	0.41
Reference simulation	36	1673	04h40	175	0.84
Uniform soil US 607	48	1696	04h30	156	0.75
Vertically homogeneous soil	38	1674	04h30	170	0.82

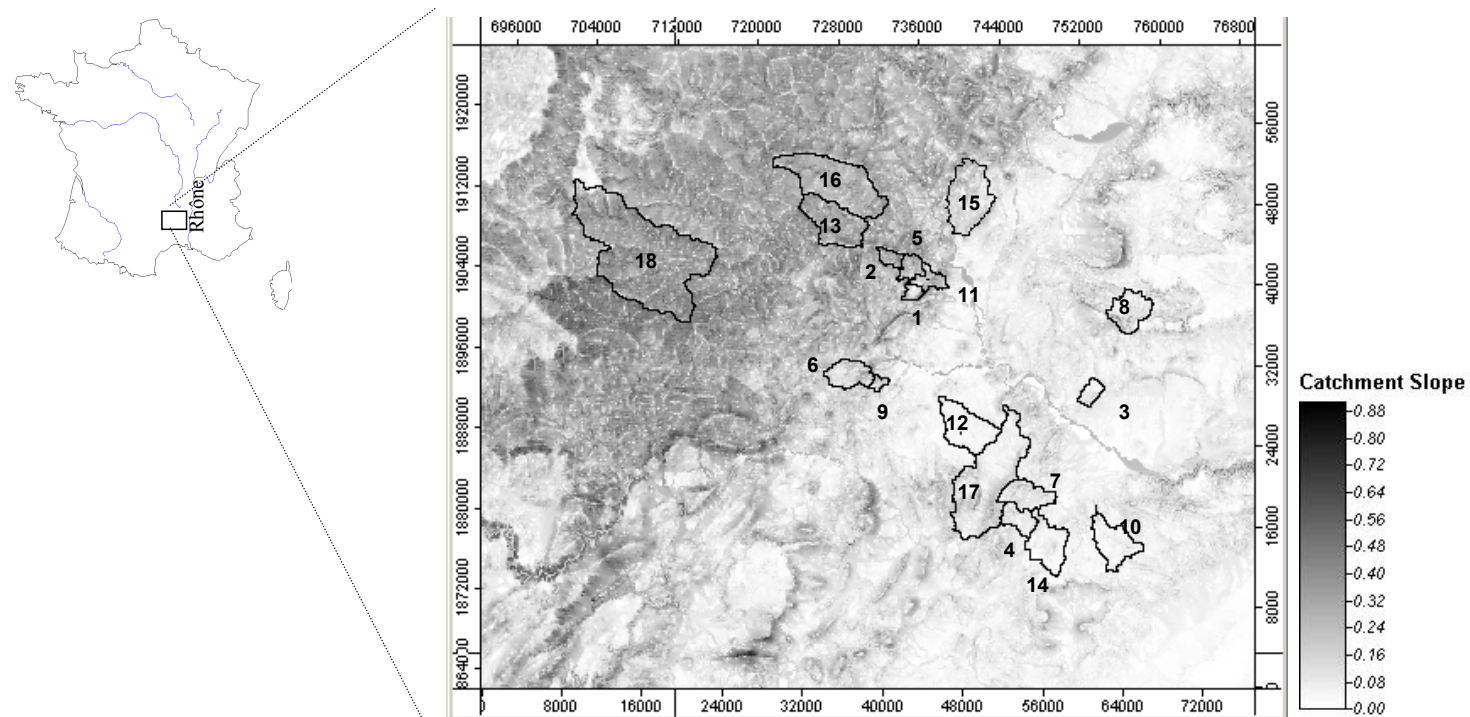


Figure 1.

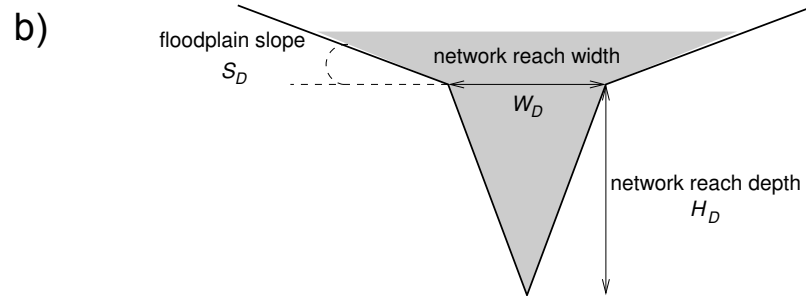
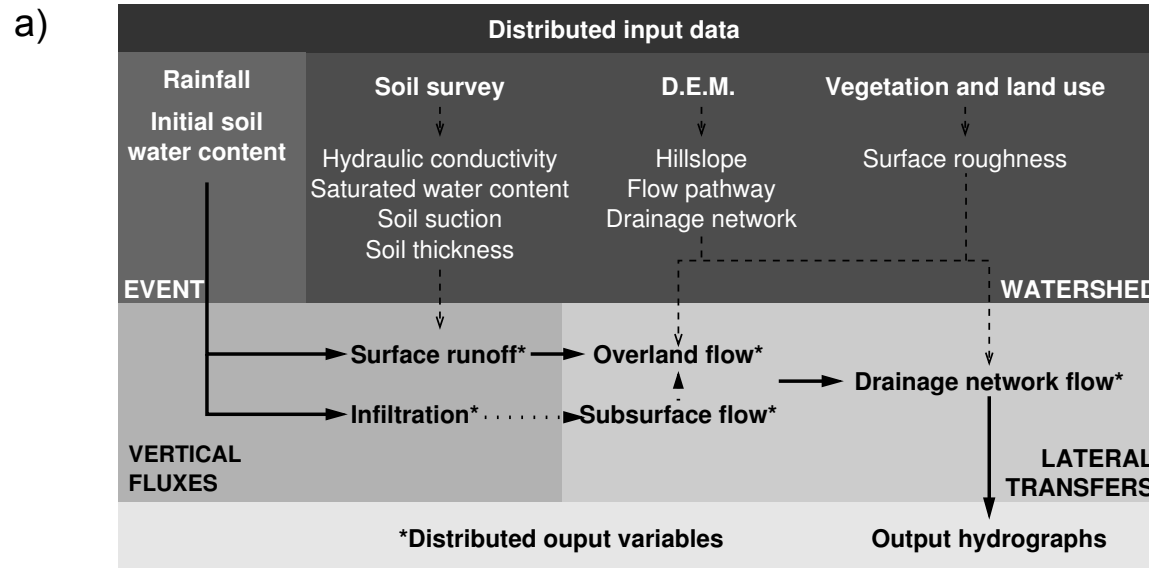


Figure 2

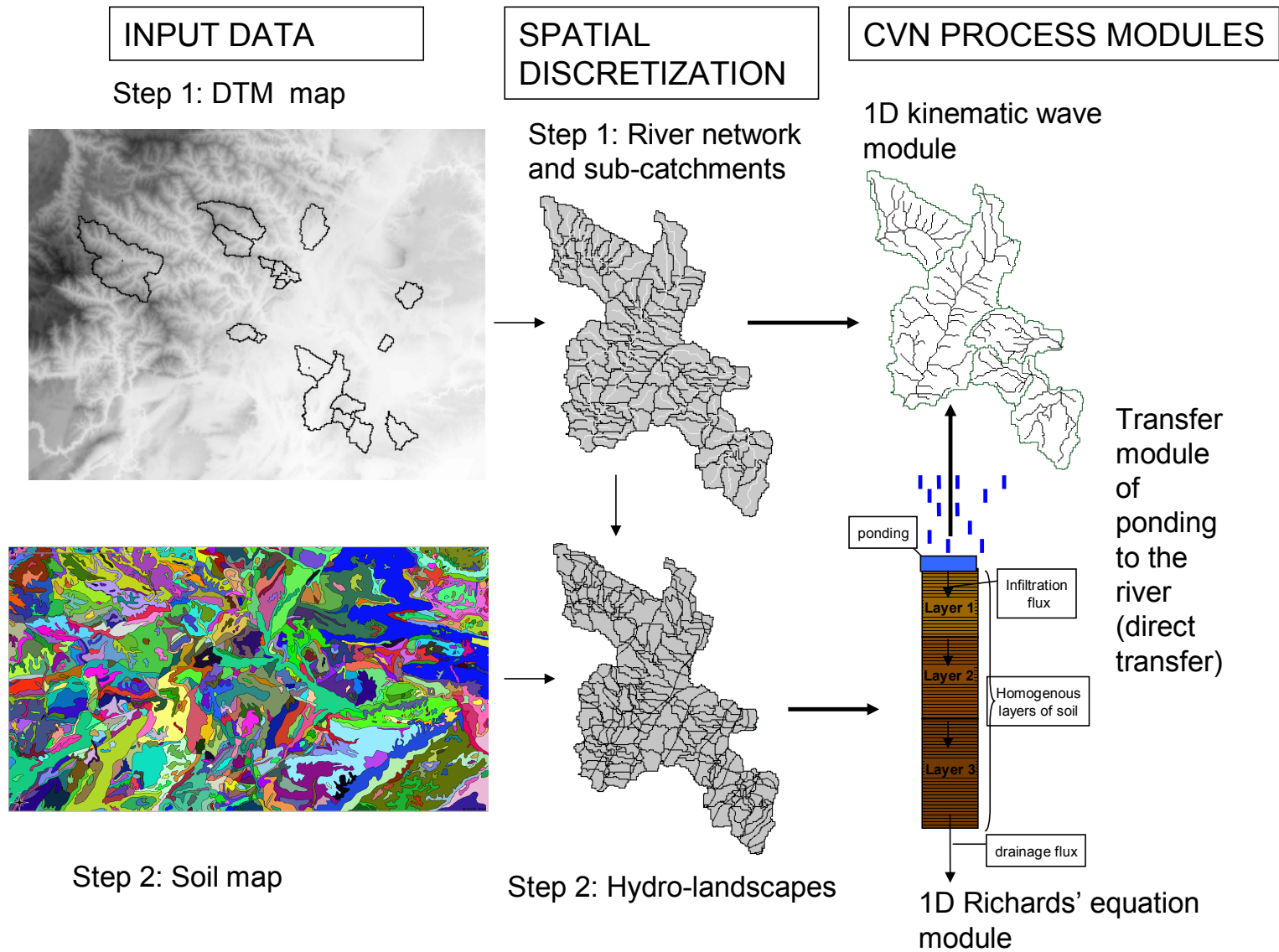


Figure 3

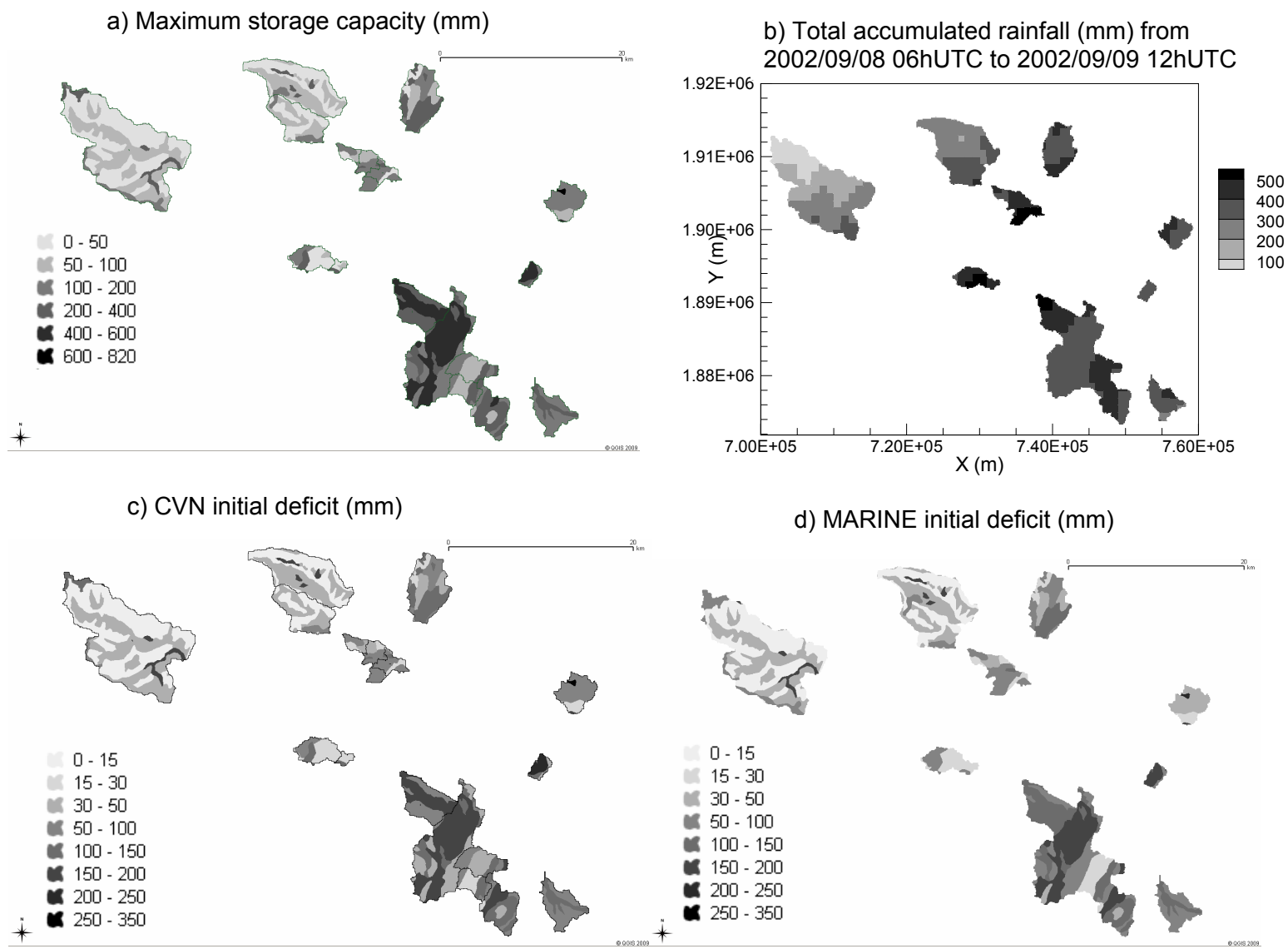


Figure 4

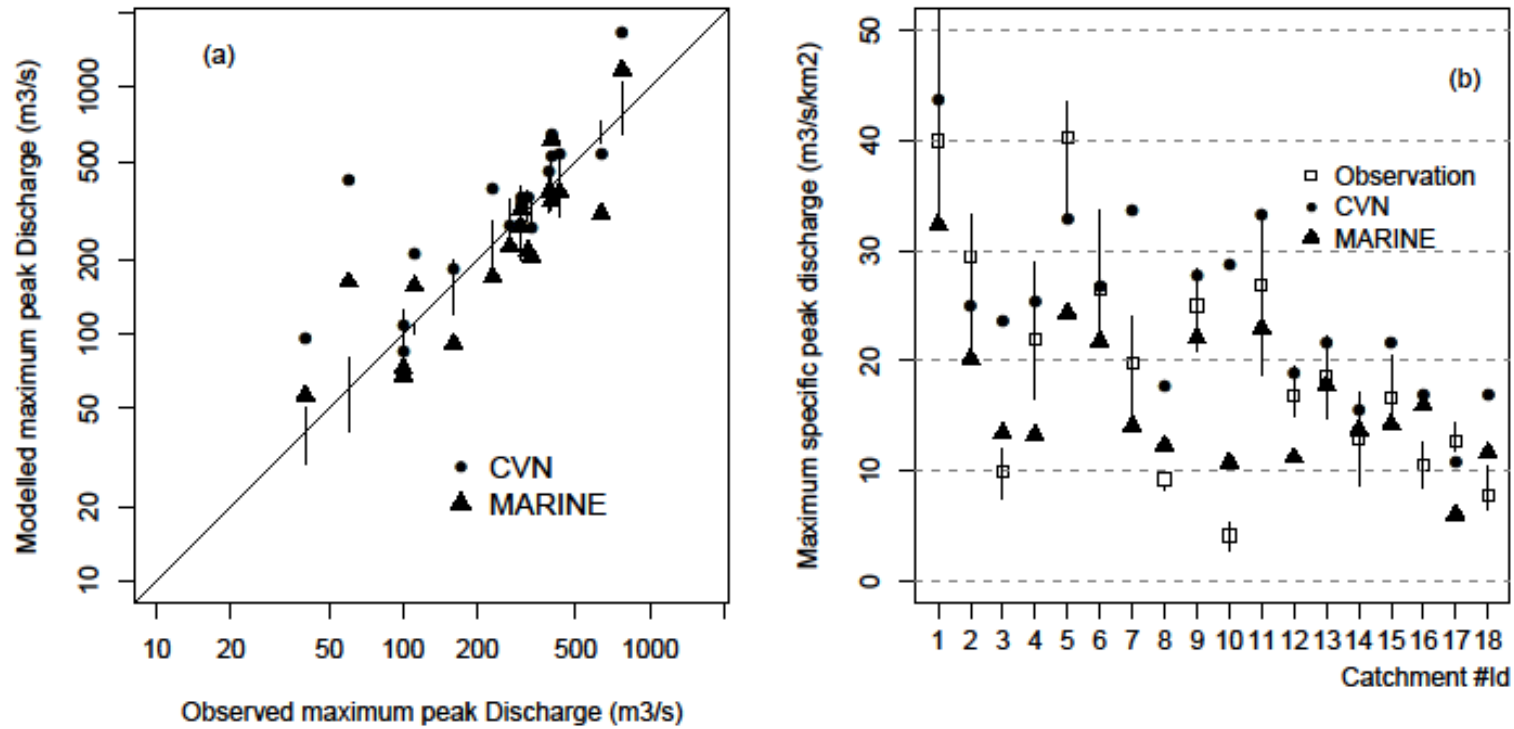


Figure 5

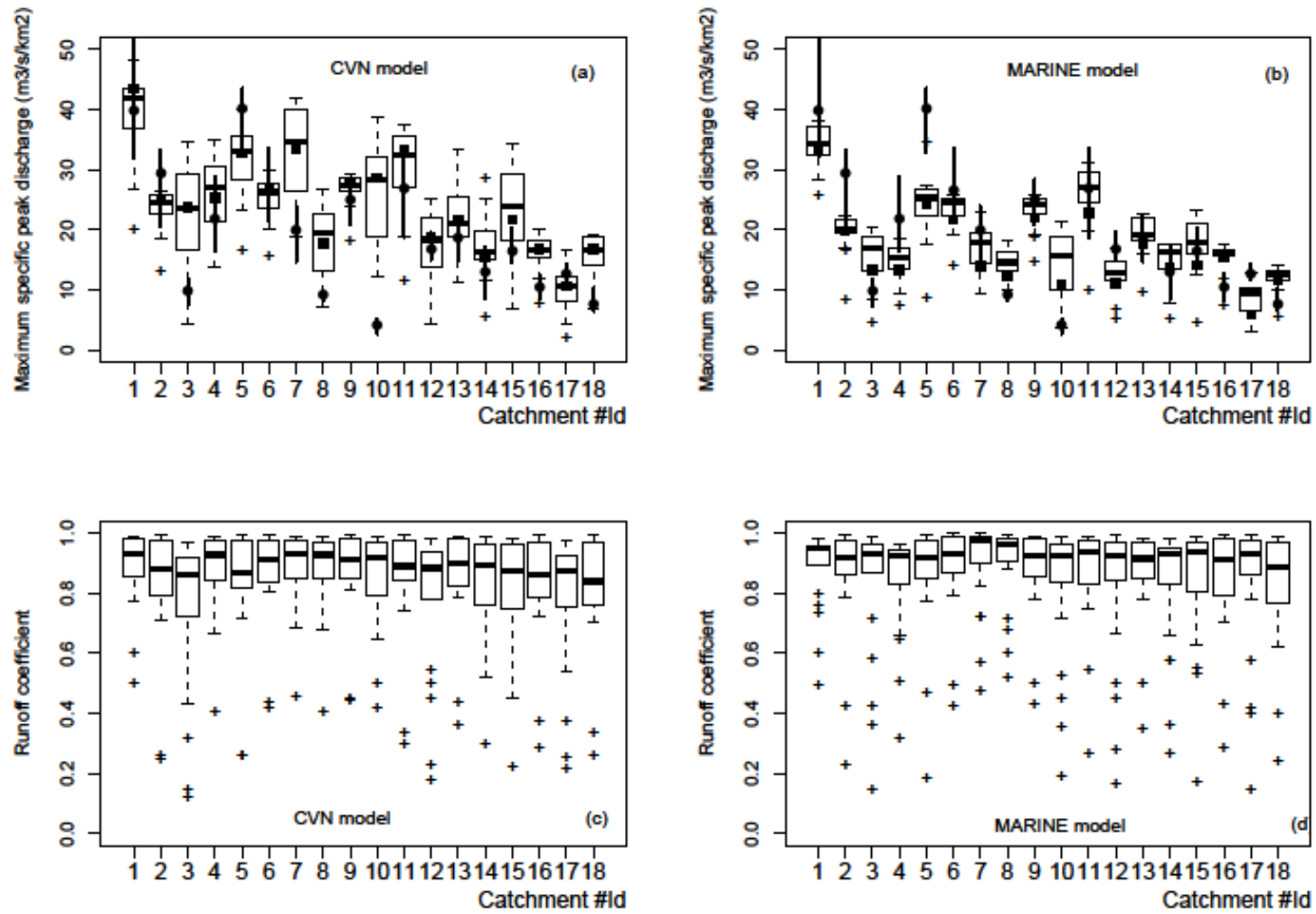


Figure 6

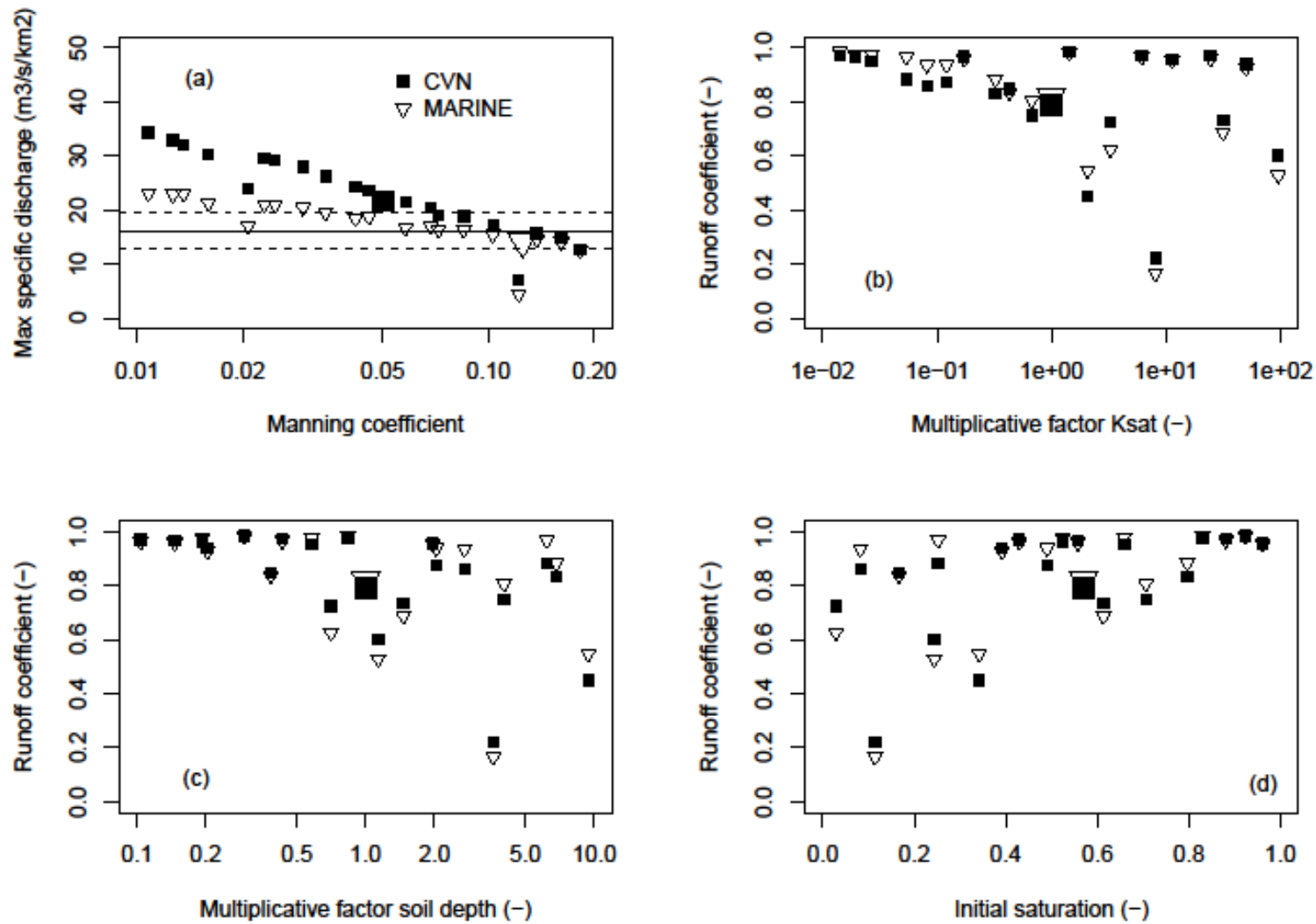


Figure 7

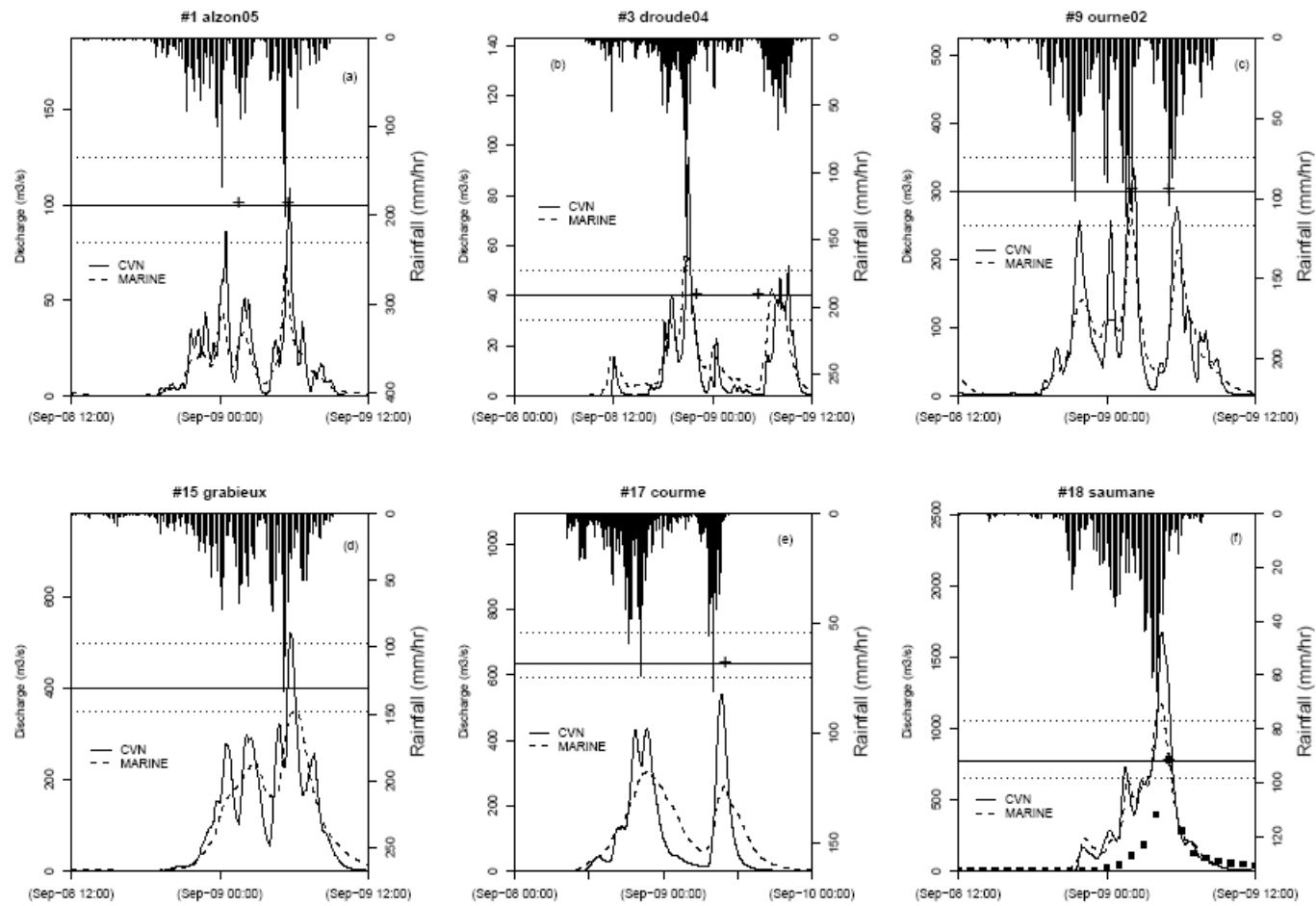


Figure 8

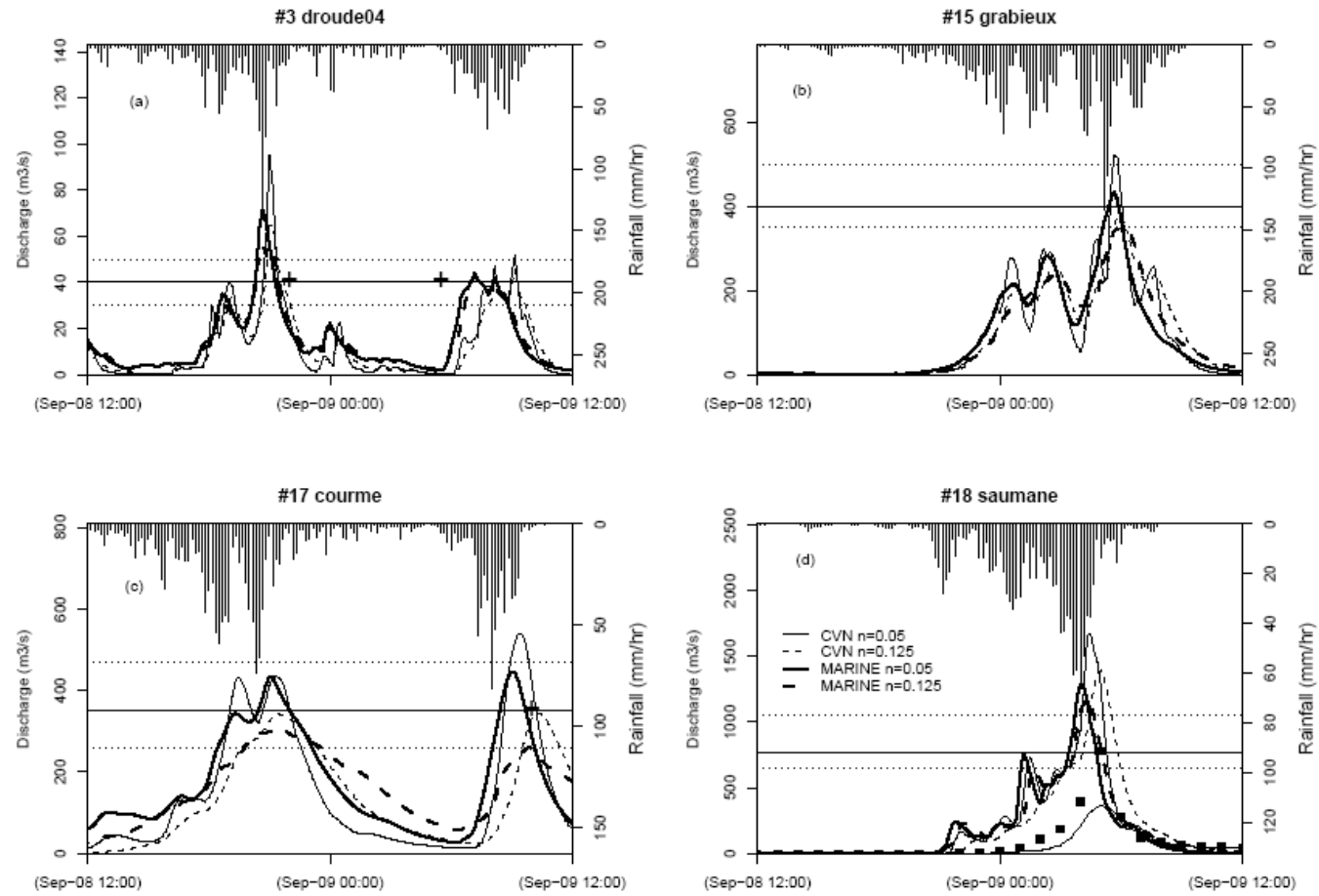


Figure 9

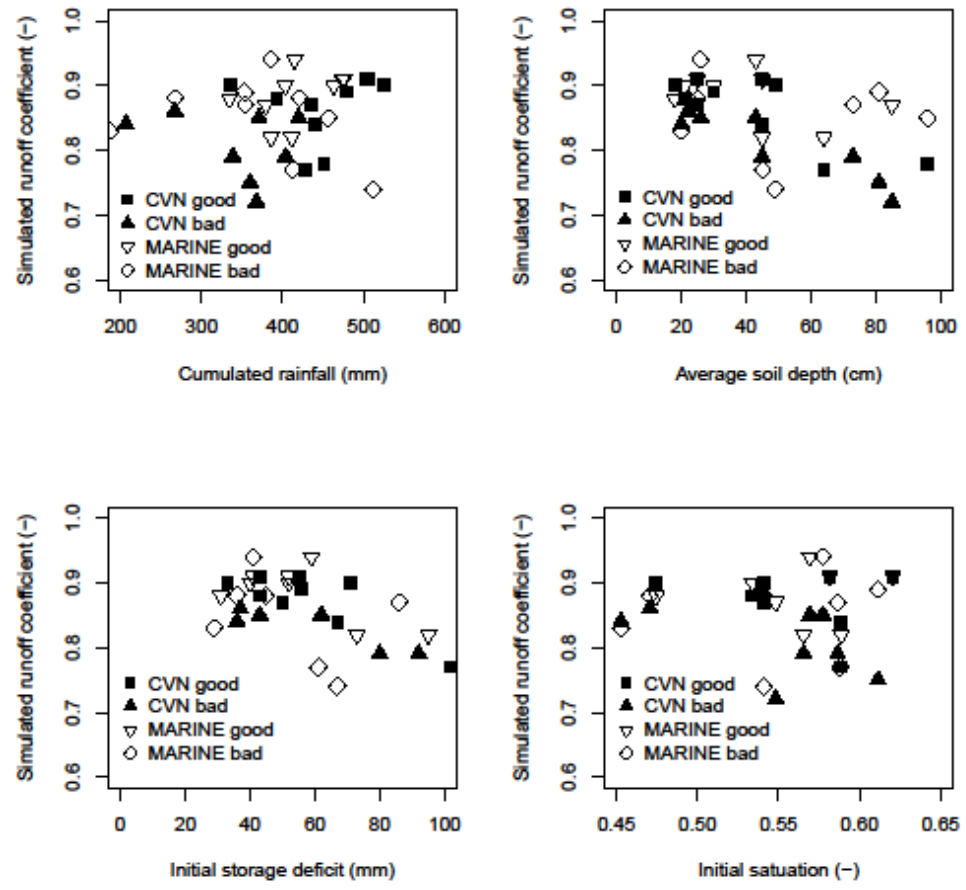


Figure 10

Figure 10. Spatial distribution and time evolution of the saturation state of each catchment with a) CVN model b) MARINE model

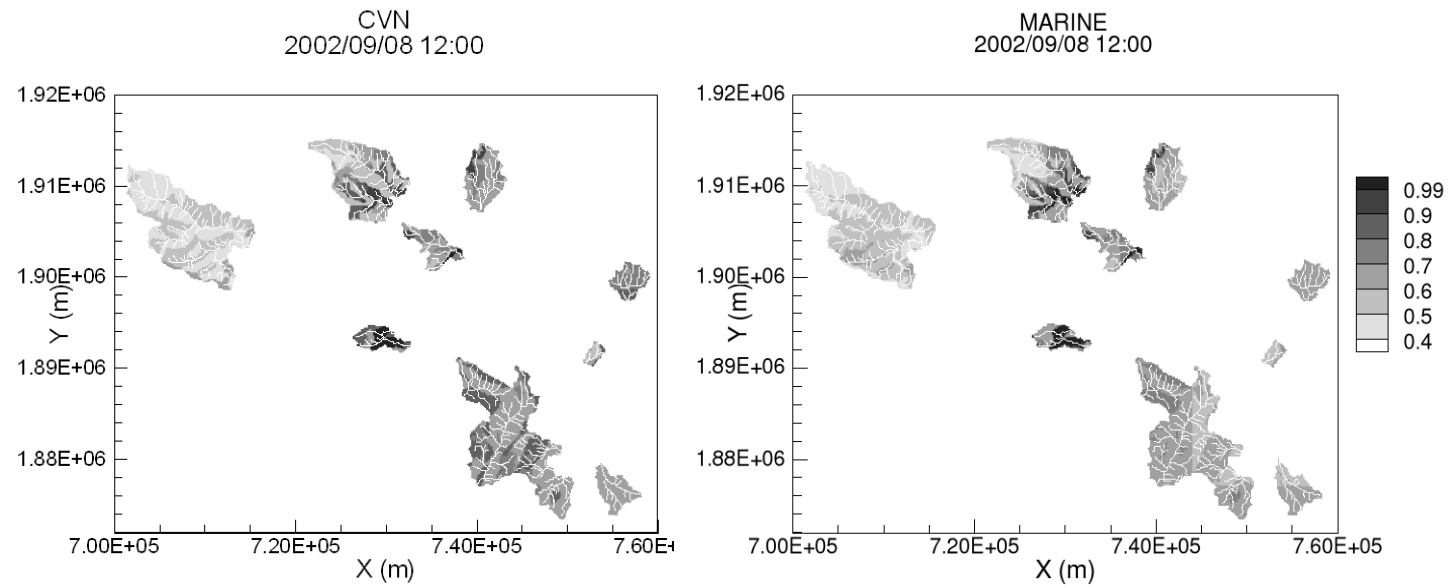


Figure 11

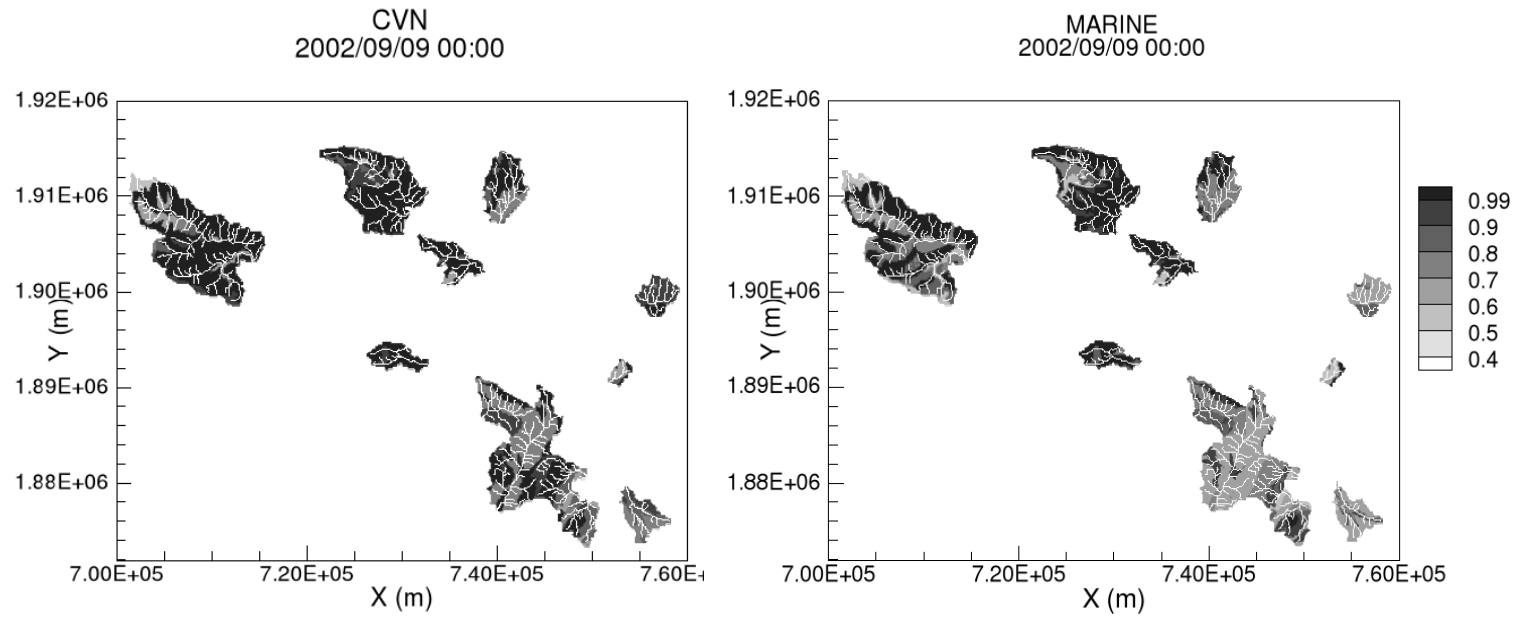


Figure 11 Continued

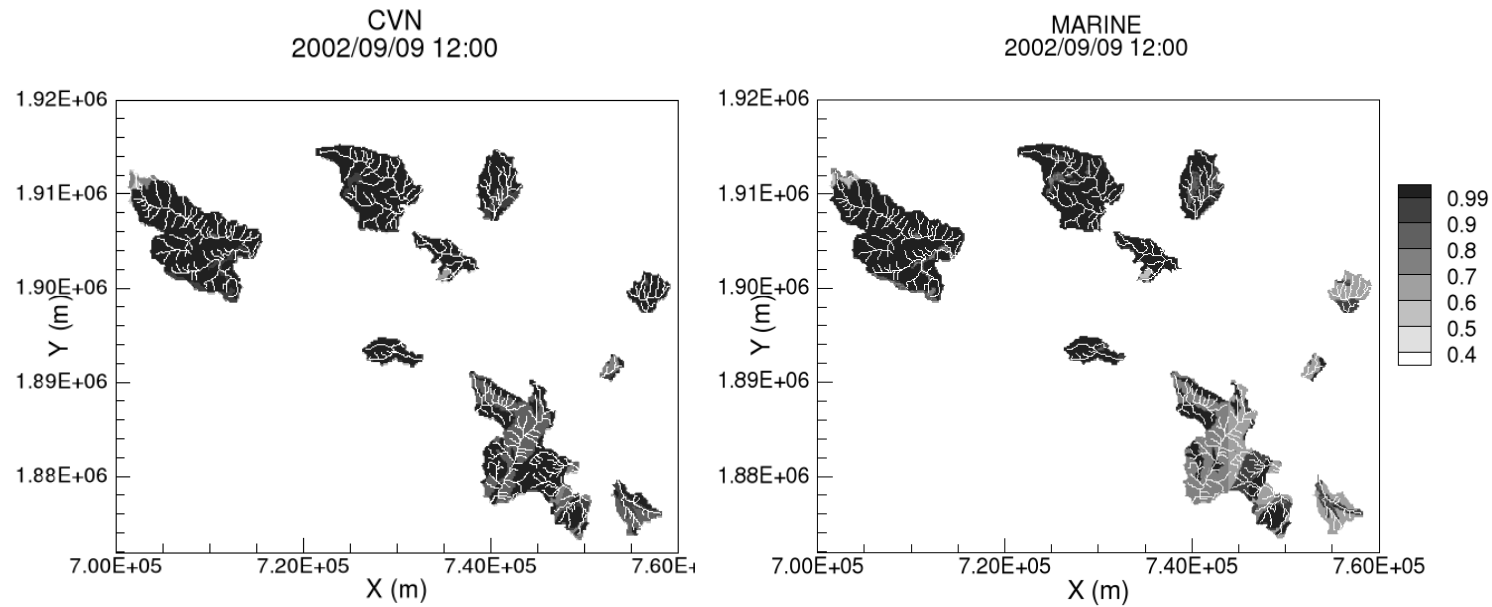


Figure 11 Continued

Figure 9. Time evolution of the mean saturation state of all the studied area

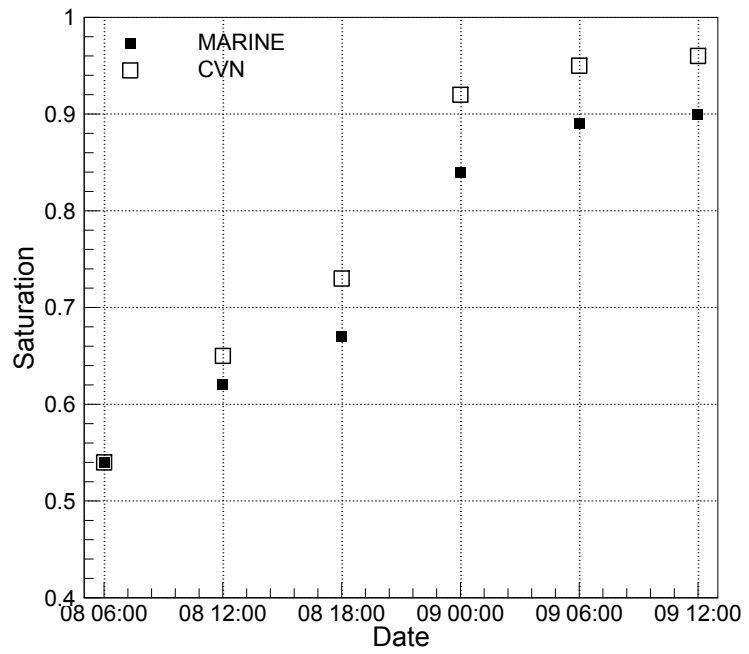


Figure 12

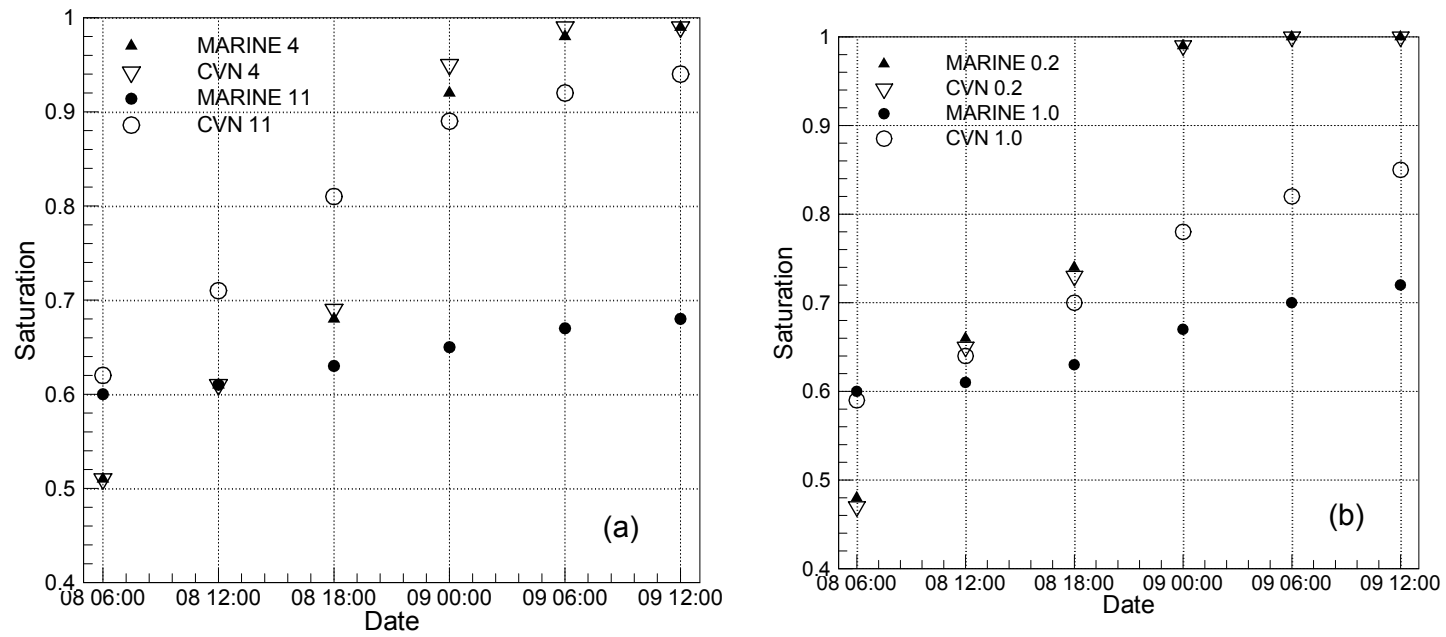


Figure 13

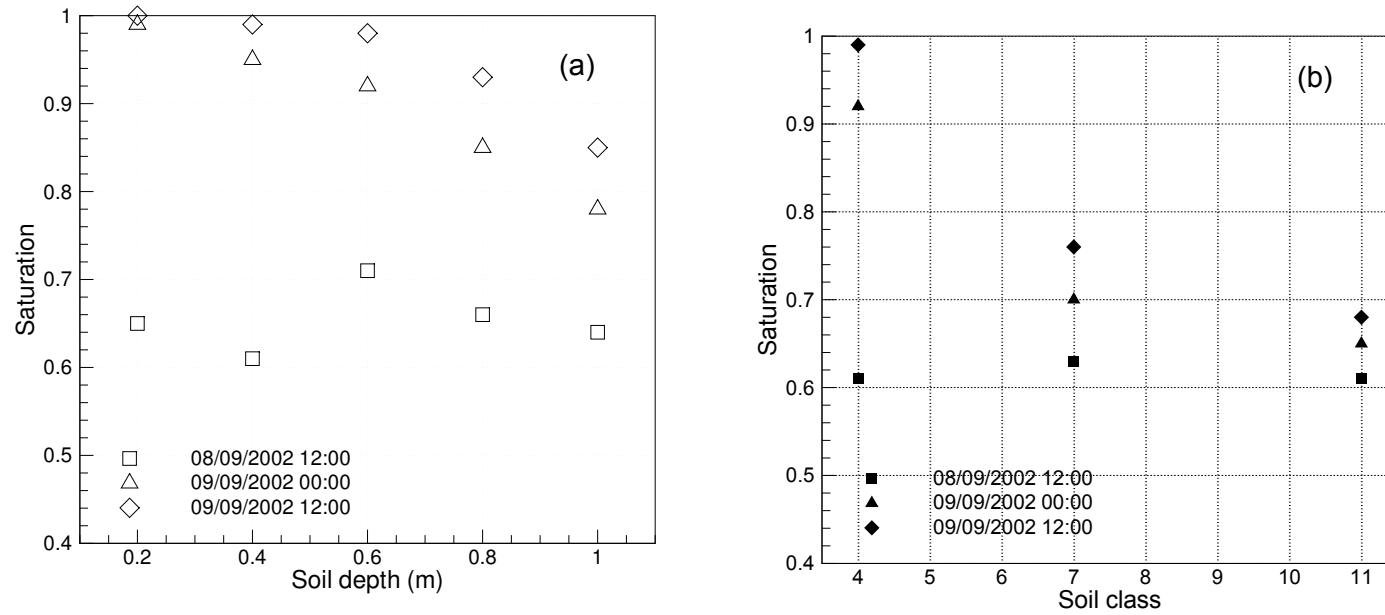


Figure 14

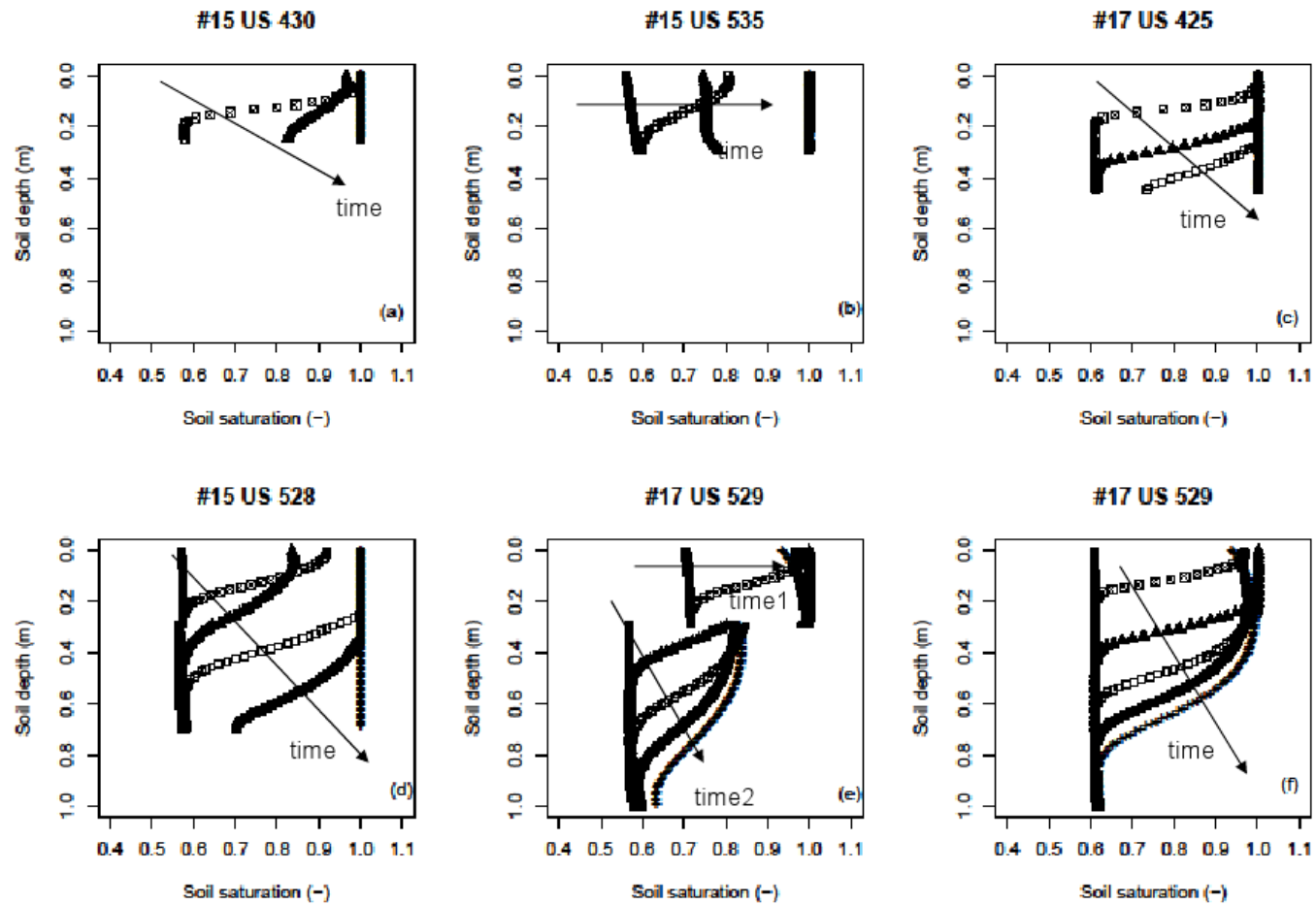


Figure 15

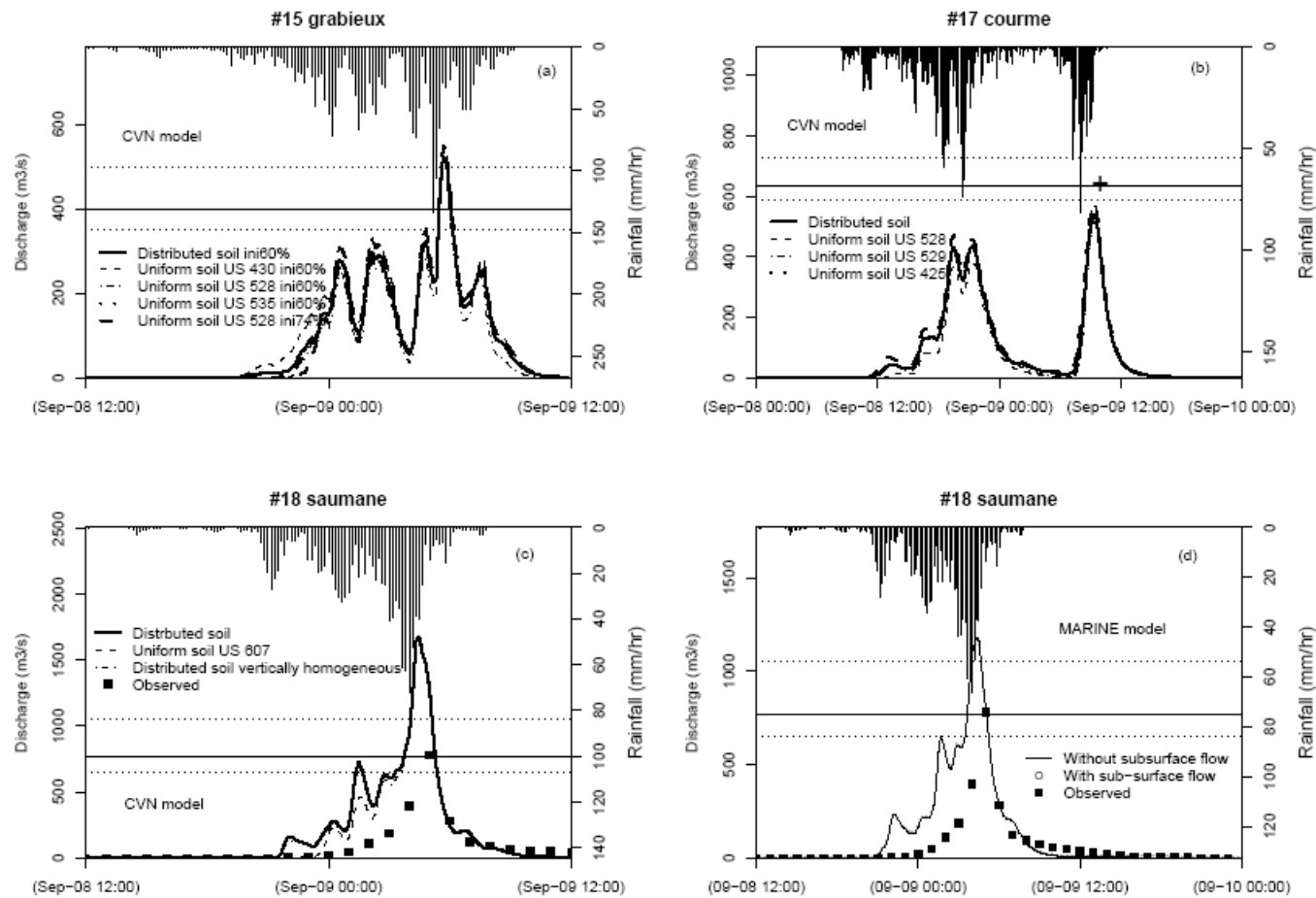


Figure 16

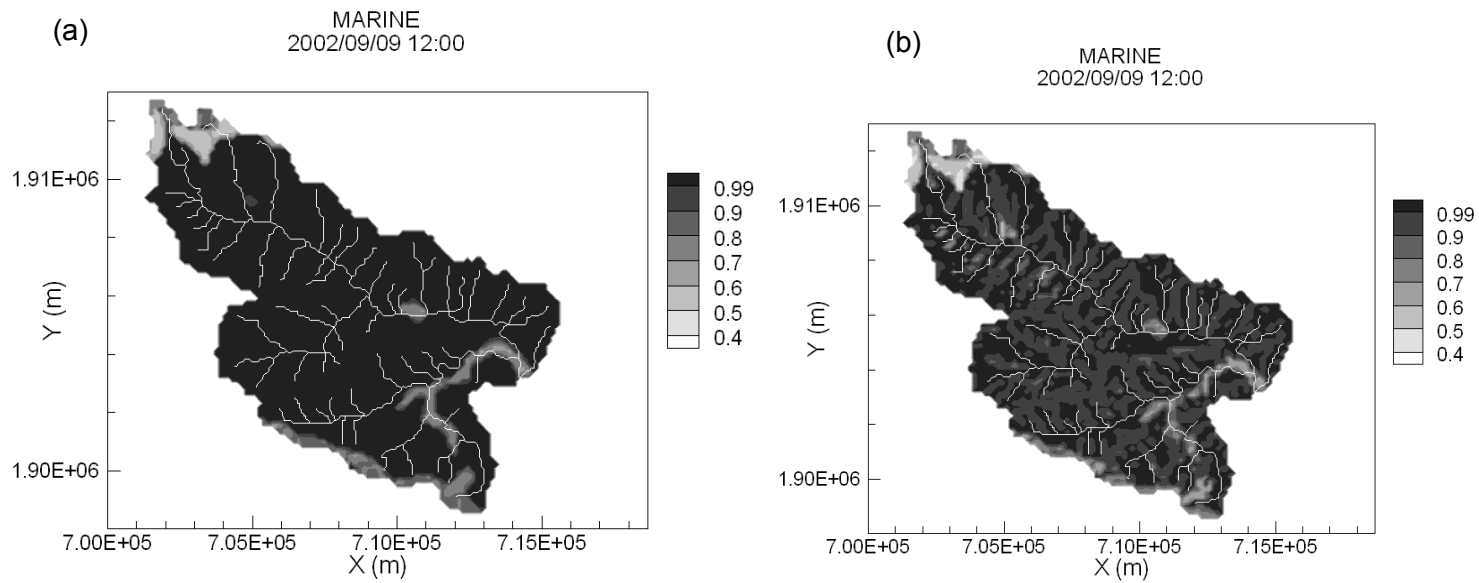


Figure 17